

THEORETICAL DEVELOPMENT
OF
IMPLICIT DYNAMIC ROUTING MODEL

D. L. Fread

Hydrologic Research Laboratory
Office of Hydrology
National Weather Service, NOAA
Silver Spring, Maryland

December 1976

revised November 1978

Presented at: Dynamic Routing Seminar
Lower Mississippi River Forecast Center
Slidell, Louisiana
December 13-17, 1976

PREFACE

This report is the second of a series describing the use of the complete equations of unsteady flow for real-time computation of stages and discharges in rivers, reservoirs, and estuaries that are forecast by the National Weather Service. The first report, NOAA Technical Memorandum NWS HYDRO-18, "Numerical Properties of Implicit Four-Point Finite Difference Equations of Unsteady Flow," examined the numerical properties of the implicit difference scheme utilized in the "implicit dynamic routing model," presented in this report.

CONTENTS

List of figures	v
Abstract	vii
1. Introduction	1-1
2. Derivation of the Saint-Venant equations	2-1
Introduction	2-1
Conservation of mass	2-1
Conservation of momentum	2-4
The Saint-Venant equations	2-11
3. Solution methods of the Saint-Venant equations	3-1
Introduction	3-1
Method of characteristics	3-1
Development of characteristic equations	3-1
First-order finite-difference approximation	3-6
Computation of interior points	3-8
Initial conditions	3-9
Boundary conditions	3-9
Finite-difference approximations	3-14
Explicit finite-difference methods	3-19
Implicit finite-difference methods	3-23
4. Weighted four-point implicit method	4-1
Introduction	4-1
Numerical properties	4-2
Finite-difference equations	4-9
Boundary and initial conditions	4-12

Solution of system of difference equations	4-18
Relaxation algorithm for system of rivers	4-25
References	R-1
Appendix A. Solution of non- linear equation by Newton- Raphson iteration	A-1
Appendix B. Solution of non-linear system of equations by Newton-Raphson iteration	B-1
Appendix C. Compact Gaussian elimination algorithm for quad-diagonal systems	C-1

LIST OF FIGURES

Figure		Page
2.1	Profile and cross-section of an elemental reach of channel	2-2
2.2	Forces acting on surface of control volume	2-5
3.1	Characteristic curves in the x-t plane	3-5
3.2	Characteristic net in x-t plane	3-7
3.3	Domain of dependence for point T	3-10
3.4	Range of influence of point M	3-11
3.5	Characteristic net with initial points	3-12
3.6	Derivation of finite difference approximations for derivatives	3-15
3.7	Finite difference approximations for explicit diffusion scheme	3-18
3.8	Weighted four-point implicit scheme	3-25
3.9	Weighted six-point implicit scheme	3-27
4.1.a	Damping convergence ratio, C_d , against D_L , for box scheme with variations in D_c and $D_f = 0.0$	4-6
4.1.b	Celerity convergence ratio, C_c , against D_L for box scheme with variations in D_c and $D_f = 0.0$	4-6
4.2.a	Damping convergence ratio, C_d , against D_L for backward implicit scheme with variations in D_c and $D_f = 0.0$	4-7
4.2.b	Celerity convergence ratio, C_c , against D_L for backward implicit scheme with variations in D_c and $D_f = 0.0$	4-7
4.3.a	Damping convergence ratio, C_d , against D_L for box scheme with variations in D_c and $D_f = 1.0$	4-8
4.3.b	Celerity convergence ratio, C_c , against D_L for box scheme with variations in D_c and $D_f = 1.0$	4-8

4.4	x-t solution plane showing time lines, nodes, grids, upstream and downstream boundaries, and initial condition time line	4-13
4.5	Single-value rating curve	4-16
4.6	Loop rating curve	4-16
4.7	Application of implicit solution technique to system of rivers	4-26
A-1	Graphical illustration of convergence process of Newton-Raphson iteration	A-3

ABSTRACT

The theoretical development of an implicit dynamic routing model is presented. The model, which is being implemented by the National Weather Service on major waterways forecast for flood warnings and other flow conditions, is based on the one-dimensional differential equations of unsteady flow known as the Saint-Venant equations. These equations consist of an equation of continuity which conserves the mass of the flow and an equation of momentum which conserves the flow momentum. This report presents a detailed derivation of the equations. Also, finite difference techniques such as the characteristic, explicit, and implicit methods of solving the equations are discussed. An implicit method known as the weighted four-point implicit method is selected for reasons of its versatility and desirable numerical properties of stability and convergence and is presented in detail.

1. INTRODUCTION

The accuracy of real-time predicted water surface elevations or stages for unsteady flows in reservoirs, estuaries, and major rivers and their tributaries is becoming increasingly important as population growth increases along the major waterways. In order to provide better river forecasts of impending floods as well as other flow conditions, the National Weather Service is in the process of implementing a new method of predicting the flow and stages in major waterways that are forecast as a service to the general public including commercial riverine interests pertaining to navigation, power, and recreation. The new forecast method, "implicit dynamic routing," is a mathematical model based on the complete one-dimensional differential equations of unsteady flow. These are known as the "Saint-Venant equations," after Barré de Saint-Venant who first derived them in 1871.

Unsteady flow in rivers, reservoirs, and estuaries is caused by the motion of long waves such as flood waves, tides, storm surges, and reservoir releases. This motion can be considered one-dimensional, i.e., the accelerations and velocity components of the wave in the transverse and vertical directions are neglected since they are small relative to the components in the direction of the longitudinal axis of the waterway. Hence, the wave motion may be adequately described by the one-dimensional Saint-Venant equations which consist of a continuity equation which conserves the mass of the flow and a momentum equation which conserves the flow momentum.

Due to the complexity of the Saint-Venant equations, solutions of the complete equations were impractical until the advent of computers; however, extensive developments in numerical analysis techniques for obtaining accurate and computationally feasible solutions to the equations were also necessary before dynamic routing could become a practical prediction technique. Computer development has now progressed to the third and fourth generation computers and numerical solution techniques have been sufficiently developed to make dynamic routing a practical and feasible technique for operational forecasting of the unsteady flows in major waterways. For example, the stages and discharges along a 400-mile river system can be forecast for a 90-day duration flood in approximately 10-20 seconds of third generation computer time. As computers continue to be developed having greater computational efficiency and storage capabilities, the feasibility of using dynamic routing will become even greater.

Existing operational streamflow forecast techniques which were developed prior to computer availability were based on gross simplifications of the unsteady flow equations. The continuity equation was retained and the momentum equation was greatly simplified to include only the effects of frictional resistance while the effects of flow accelerations and water surface slope were ignored. When these ignored effects are important, the accuracy of predicted stages and discharges

can be increased by using dynamic routing. The neglected effects are of critical importance in cases of: (1) upstream movement of waves such as tides and storm surges, (2) backwater effects produced by downstream reservoirs and tributary inflows, (3) typical flood waves in waterways having channel bottom slopes less than approximately 2-3 feet per mile, and (4) abrupt waves caused by controlled releases from reservoirs or by the catastrophic failure of dams.

The dynamic routing model also provides additional hydraulic information about flow along the waterways such as the depth, flow cross-sectional area and top width, hydraulic radius, velocity, water surface slope, and energy slope. This information is necessary for predicting sediment transport along the waterway. The transport of sediment affects the channel bed elevation through the processes of degradation (scour) and aggradation (deposition or fill). In some rivers, bed elevation changes are significant enough to seriously affect the stages. Also, channel resistance in sand-bed rivers is affected by sediment transport which causes changes in the form or shape of the sand waves along the bottom of the river. Such changes result in changes in flow resistance which can be significant enough to seriously affect the river stages. Also, the hydraulic information provided by the dynamic routing model is required to forecast water temperature changes along the waterway.

The dynamic routing model also provides advantages over simpler techniques when forecasting extreme flood events that exceed previous flow records, such as those resulting from a record rainfall or a dam failure. A technique such as dynamic routing which neglects fewer of the essential physical processes characterizing the flood wave propagation phenomenon, relies less on previous flow records than do simplified techniques. Thus, it may be used with less error to predict extreme flows as fewer of the significant factors affecting the flood wave need to be extrapolated beyond previous experience.

Dynamic routing was first used by Stoker [1953] and Isaacson, et al. [1954] in their pioneering investigation of flood routing in the Ohio River and has since been modified and applied by many investigators. This report presents the theoretical development of the implicit dynamic routing model currently being implemented by the National Weather Service. A detailed derivation of the Saint-Venant equations is presented to provide insight into the physical basis of the model. The numerical solution technique, an implicit finite difference numerical integration scheme, is presented in detail. Also, a brief development of two other solution techniques, the "method of characteristics" and the "explicit method," are presented to provide useful background information for understanding the mathematical concepts, complexities, and advantages associated with the implicit numerical integration technique.

2. THE SAINT-VENANT EQUATIONS: THEIR DERIVATION AND RELATION TO OTHER FLOW-ROUTING METHODS

Introduction

The mechanics of the unsteady open-channel flow of water may be expressed mathematically in terms of the Saint-Venant equations. These equations are partial differential equations which may be derived from the laws of conservation of mass and momentum. Various derivations have been presented, e.g., Stoker [1957], Chow [1959], Henderson [1966], Streeter and Wylie [1967], Strelkoff [1969], Liggett [1975], and many others.

It is assumed in the derivation that the flow is one-dimensional in the sense that flow characteristics such as depth and velocity are considered to vary only in the longitudinal x-direction of the channel. It is further assumed that: (1) the velocity is constant and the water surface is horizontal across any section perpendicular to the longitudinal axis; (2) the flow is gradually varied with hydrostatic pressure prevailing at all points in the flow such that the vertical acceleration of water particles may be neglected; (3) the longitudinal axis of the channel can be approximated by a straight line; (4) the bottom slope of the channel is small; (5) the bed of the channel is fixed, i.e., no scouring or deposition is assumed to occur; (6) the resistance coefficient for steady uniform turbulent flow is considered applicable, and an empirical resistance equation such as the Manning equation describes the resistance effects; and (7) the flow is incompressible and homogeneous in density.

Conservation of Mass

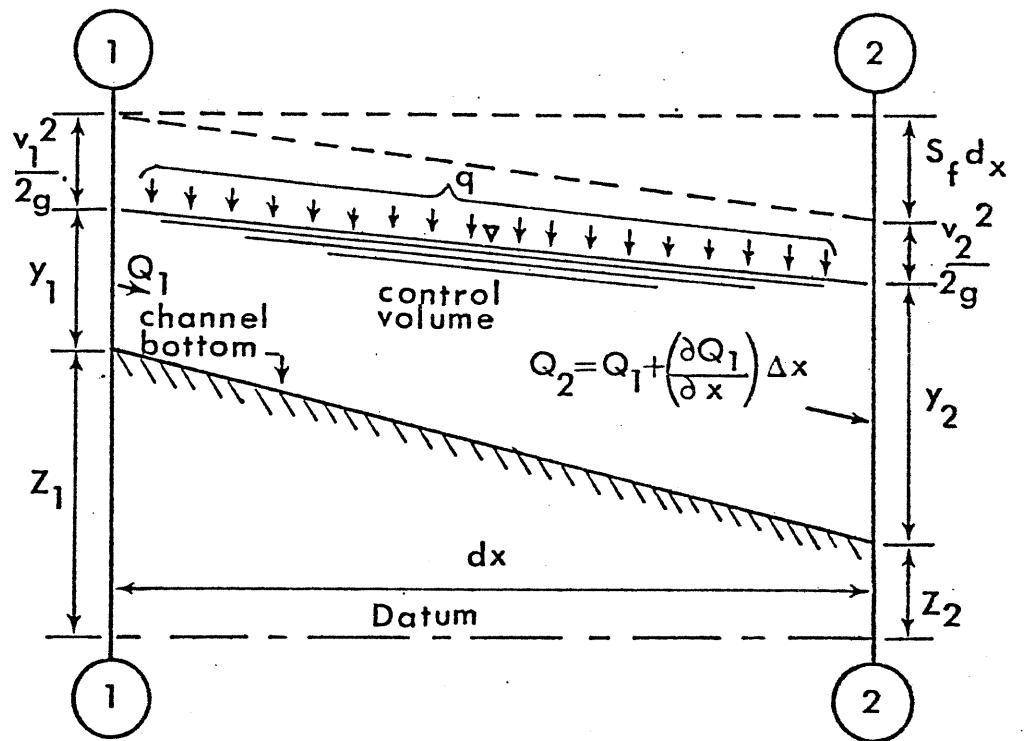
The law of conservation of mass is used to derive the first of the Saint-Venant equations, i.e., the equation of continuity. Conservation of mass simply expresses the fact that mass inflow minus mass outflow equals the time rate of change of mass stored within the channel volume being considered.

Consider a control volume of channel of length dx with flow proceeding from section 1 to section 2, as shown in Fig. 2.1. Let x be the horizontal distance, positive being taken in the downstream direction; ρ , the density of water; g , the gravity acceleration constant; z , the elevation of the channel bottom above a datum plane; y , the depth of water; A , the cross-sectional area; V , the average velocity; and B , the width of the free surface. The depth at section 1 is y and at section 2 is $y+(\partial y/\partial x)dx$. The cross-sectional area is A at section 1 and $A+(\partial A/\partial x)dx$ at section 2. Let ρQ be the mass flow rate entering the channel through section 1; $\rho Q+\rho(\partial Q/\partial x)dx$, the mass outflow rate; and q , the lateral inflow per unit channel length per unit time, where q has dimensions of ft^2/sec .

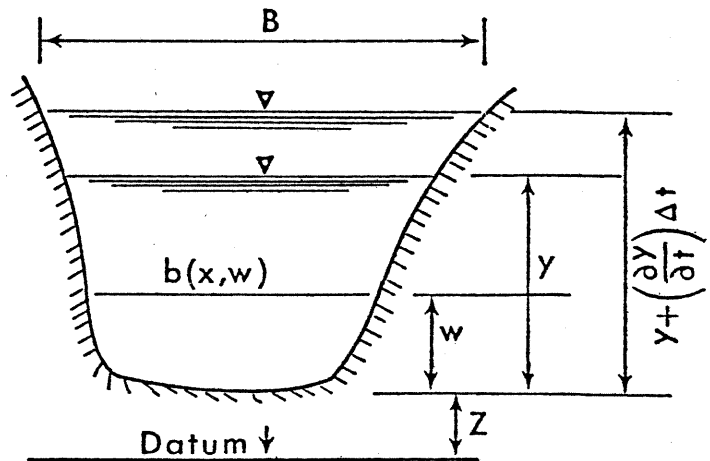
The mass inflow I_{ma} to the dx reach of channel during a time interval dt is:

$$I_{ma} = \rho(Q + q dx) dt \quad (2.1)$$

and the mass outflow O_{ma} from the same dx reach during the time interval



PROFILE



CROSS-SECTION

Fig. 2.1.--Profile and cross-section of an elemental reach of channel.

dt can be expressed as:

$$O_{ma} = \rho [Q + (\partial Q / \partial x) dx] dt \quad (2.2)$$

If $\partial Q / \partial x$ is taken as positive, there is a net mass outflow from the reach. The mass of water remaining within the dx reach is simply the product of the elemental volume times the mass density, and the time rate of change of this mass (dS_{ma} / dt) during a dt interval of time may then be expressed in the form:

$$\frac{dS_{ma}}{dt} = \frac{\partial(\rho A \cdot dx)}{\partial t} dt \quad (2.3)$$

Now, according to the law of conservation of mass, the mass inflow minus the mass outflow must equal the time rate of change of mass storage within the reach, i.e.,

$$I_{ma} - O_{ma} = \frac{dS_{ma}}{dt} \quad (2.4)$$

or:

$$\rho(Q + q dx) dt - \rho(Q + \frac{\partial Q}{\partial x} dx) dt = \frac{\partial(\rho A dx)}{\partial t} dt \quad (2.5)$$

Upon simplifying Equation (2.5), one obtains:

$$\partial Q / \partial x + \partial A / \partial t - q = 0 \quad (2.6)$$

which is known as the conservation form of the equation of continuity for a prismatic or non-prismatic channel. Sometimes the second term of Equation (2.6) is expressed as the sum of the active channel area and the dead storage area A_0 , wherein the velocity of flow in the x-direction is considered negligible such as a tributary which stores the flood waters of the main river or a heavily vegetated flood plain. In this case, Equation (2.6) is expressed in the form:

$$\partial Q / \partial x + \partial(A + A_0) / \partial t - q = 0 \quad (2.7)$$

Since $Q = AV$, $\partial A / \partial t = B \partial y / \partial t$, and for a prismatic channel, $dA = B dy$, then Equation (2.6) may be written as:

$$V(\partial y / \partial x) + A/B(\partial V / \partial x) + \partial y / \partial t - q/B = 0 \quad (2.8)$$

However, if the channel is non-prismatic, A is also a function of x, such that $\partial A / \partial x = (\partial A / \partial x)_y + B \partial y / \partial x$, where the subscript indicates the depth is to be held constant when taking the derivative. Then, Equation (2.8) becomes:

$$V \frac{\partial y}{\partial x} + \frac{A}{B} \frac{\partial V}{\partial x} + \frac{\partial y}{\partial t} + \frac{V}{B} \left(\frac{\partial A}{\partial x} \right)_y - \frac{q}{B} = 0 \quad (2.9)$$

Equations (2.8) and (2.9) are the non-conservation form of the equation of continuity for prismatic and non-prismatic channels, respectively. The non-conservation form enables certain finite difference solution techniques to be applied. However, the conservation form, Equations (2.6) and (2.7), is the form which will be used herein.

Conservation of Momentum

The law of conservation of momentum is used to derive the second Saint-Venant equation, i.e., the equation of motion or dynamic equilibrium. The conservation of momentum is given by Newton's second law of motion, which states: The sum of the forces acting on the surface of the control volume + the net rate of momentum entering the control volume = the time rate of accumulation of momentum within the control volume.

The forces acting on the surface of the control volume of Fig. 2.2 include: (1) the gravity force due to the weight of the fluid, (2) the force due to the frictional resistance along the channel bottom and sides, (3) the force due to the shear stress produced by wind movement at the free surface of the control volume, and (4) the unbalanced pressure force.

1. Gravity force. The force component of the weight of fluid in the control volume in the direction of the x-axis (positive if directed downstream) is:

$$F_g = \rho g A dx \sin \phi \quad (2.10)$$

However, since the angle ϕ between the channel bottom and horizontal x-axis is small, then:

$$\tan \phi \approx \sin \phi \quad (2.11)$$

and

$$\tan \phi = -\frac{dz}{dx} = S_o \quad (2.12)$$

Therefore, Equation (2.10) can be expressed as:

$$F_g = \rho g A S_o dx \quad (2.13)$$

2. Frictional force. The frictional resistance is manifested by a shear stress τ along the bottom and sides of the control volume. An empirical equation for open channel resistance such as the Chezy equation or the Manning equation can be used to express the frictional resistance. Herein, only the Manning equation is used, which is expressed by the following relationship:

$$V = \frac{1.486}{n} R^{2/3} S_f^{1/2} \quad (2.14)$$

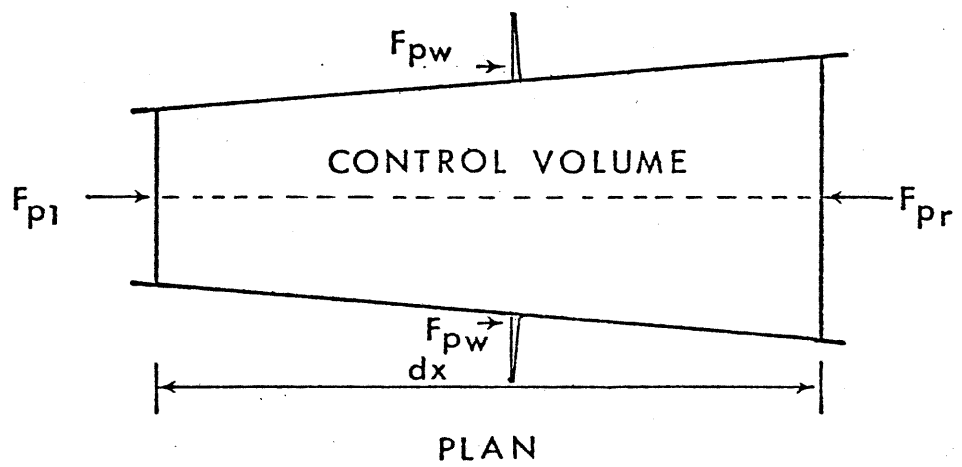
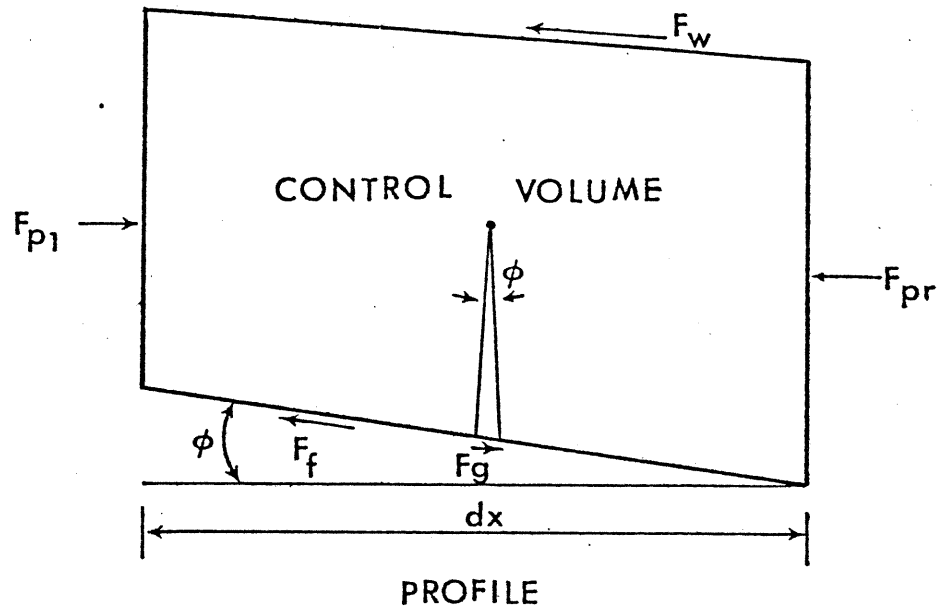


Fig. 2.2.--Forces acting on surface of control volume.

where n is the Manning resistance coefficient, which can commonly assume values ranging from 0.01 to 0.20; R is the hydraulic radius; and S_f is the friction slope. The frictional force due to the boundary shear stress is:

$$F_f = -\tau P dx \quad (2.15)$$

where P is the wetted perimeter such that $R = A/P$ and τ is the shear stress which can be expressed in terms of the friction slope S_f , i.e., in the case of uniform flow, the friction force is in balance with the gravity force and S_f is a good approximation of S_o . Thus:

$$\tau P dx = \rho g A S_f dx \quad (2.16)$$

Therefore:

$$\tau = \rho g R S_f \quad (2.17)$$

Substituting Equation (2.16) into Equation (2.15), the following expression for the frictional force is obtained:

$$F_f = -\rho g A S_f dx \quad (2.18)$$

3. Wind shear force. The force due to the shear stress at the free surface of the control volume due to the frictional resistance of wind against the surface of the flowing water is given by:

$$F_w = -\tau_w B dx \quad (2.19)$$

where B is the width of the free surface of the control volume and τ_w is the wind shear stress. In this derivation, it is assumed the wind is opposing the flow, hence, the negative sign associated with τ_w .

4. Unbalanced pressure force. The pressure distribution is assumed to be everywhere hydrostatic, as previously mentioned. This well approximates the case where the curvature of the free surface is small as is true of most flows in open channels except those known as rapidly varied flows (flow over spillways, abrupt waves, hydraulic bores, etc.). The unbalanced pressure force is seen from Fig. 2.2 to be the resultant of the forces F_{p1} , F_{pr} , F_{pw} . The hydrostatic force acting on the left side of the control volume is:

$$F_{p1} = \int_0^y \rho g (y - w) b dw \quad (2.20)$$

The hydrostatic force acting on the right side of the control volume is:

$$F_{pr} = \left(F_{p1} + \frac{F_{p1}}{x} dx \right) \quad (2.21)$$

where $\frac{\partial F_{p1}}{\partial x}$ can be obtained from Equation (2.20) by applying the Leibnitz rule for differentiation, which yields the following expression:

$$\frac{\partial F_{p1}}{\partial x} = \int_0^y \rho g \frac{\partial y}{\partial x} b \, dw + \int_0^y \rho g (y - w) \frac{\partial b}{\partial x} \, dw \quad (2.22)$$

Since the cross sectional area is:

$$A = \int_0^y b \, dw \quad (2.23)$$

Equation (2.22) can be written as:

$$\frac{\partial F_{p1}}{\partial x} = \rho g A \frac{\partial y}{\partial x} + \int_0^y \rho g (y - w) \frac{\partial b}{\partial x} \, dw \quad (2.24)$$

If the channel is non-prismatic, i.e., it narrows or widens in the downstream direction, the banks contribute an additional pressure force F_{pw} . This force is:

$$F_{pw} = \left[\int_0^y \rho g (y - w) \frac{\partial b}{\partial x} \, dw \right] dx \quad (2.25)$$

The unbalanced pressure force F_p can be determined by summing the various pressure forces acting on the surface of the control volume. Thus:

$$F_p = F_{p1} - \left(F_{p1} + \frac{\partial F_{p1}}{\partial x} dx \right) + F_{pw} \quad (2.26)$$

or:

$$F_p = - \frac{\partial F_{p1}}{\partial x} dx + F_{pw} \quad (2.27)$$

Substituting Equations (2.24) and (2.25) in Equation (2.27) yields:

$$\begin{aligned} F_p &= -\rho g A \frac{\partial y}{\partial x} dx - dx \int_0^y \rho g (y - w) \frac{\partial b}{\partial x} \, dw \\ &+ dx \int_0^y \rho g (y - w) \frac{\partial b}{\partial x} \, dw \end{aligned} \quad (2.28)$$

Since the last two terms of Equation (2.28) cancel one another, the unbalanced pressure force is simply:

$$F_p = -\rho g A \frac{\partial y}{\partial x} dx \quad (2.29)$$

If the channel is prismatic, the second and third terms of Equation (2.28) are zero since $\partial b/\partial x = 0$ for the prismatic channels. Therefore, Equation (2.29) is applicable for prismatic channels.

The sum of all forces acting on the control volume is given by the algebraic summation of the gravity, frictional, wind shear, and unbalanced pressure forces. Thus, summing Equations (2.13), (2.18), (2.19), and (2.29), we obtain:

$$F = F_g + F_f + F_w + F_p \quad (2.30)$$

or:

$$F = \rho g A S_o dx - \rho g A S_f dx - \tau_w B dx - \rho g A \frac{\partial y}{\partial x} dx \quad (2.31)$$

The rate of flow of momentum in the x direction is the product of the mass rate of flow ρQ and the velocity component in the x direction.

The incoming flow of momentum I_{mo} includes that entering the left side of the control volume and that entering along the dx length due to the contribution of lateral inflow with a velocity in the x-direction of v_x . Thus:

$$I_{mo} = \rho(\beta VQ + \beta v_x q dx) \quad (2.32)$$

where the momentum correction factor β is applied to the velocities to account for the nonuniformity of the velocity in the vertical and horizontal directions.

The β factor is commonly assumed as 1.0, although it can range from 1.0 to 1.3, and may become significant in cases where the velocity distribution in the cross-section is greatly distorted. The assumption of uniform velocity, i.e., $\beta = 1.0$, causes no error in the continuity Equation (2.6).

The momentum outflow from the control volume is:

$$O_{mo} = \rho \left(\beta VQ + \frac{\partial(\beta VQ)}{\partial x} dx \right) \quad (2.33)$$

Therefore, the net rate of flow of momentum entering the control volume is:

$$N_{mo} = I_{mo} - O_{mo} \quad (2.34)$$

or:

$$N_{mo} = \rho \left[\beta VQ + \beta v_x q dx - \beta VQ - \frac{\partial (\beta VQ)}{\partial x} dx \right] \quad (2.35)$$

which reduces to:

$$N_{mo} = \rho \left[\beta q v_x - \frac{\partial (\beta VQ)}{\partial x} \right] dx \quad (2.36)$$

The time rate of accumulation of momentum in the control volume is simply:

$$S_{mo} = \rho \frac{\partial Q}{\partial t} dx \quad (2.37)$$

Now, upon applying the law of conservation of momentum, the momentum within the control volume is:

$$F + N_{mo} = S_{mo} \quad (2.38)$$

Substituting Equations (2.31), (2.36), and (2.37) in Equation (2.38) yields:

$$\begin{aligned} \rho g A S_o dx - \rho g A S_f dx - \tau_w B dx - \rho g A \frac{\partial y}{\partial x} dx \\ + \rho \left[\beta q v_x - \frac{\partial (\beta VQ)}{\partial x} \right] dx = \rho \frac{\partial Q}{\partial t} dx \end{aligned} \quad (2.39)$$

After dividing through by ρdx , the following is obtained:

$$\frac{\partial Q}{\partial t} + \frac{\partial (\beta VQ)}{\partial x} + g A \left(\frac{\partial y}{\partial x} - S_o + S_f \right) - \beta q v_x + \frac{\tau_w}{\rho} B = 0 \quad (2.40)$$

which is the conservation form of the equation of motion.

In many applications, particularly natural channels, such as rivers, reservoirs, and estuaries, it is convenient to replace the depth y with the water surface elevation h referenced above some datum. Since the water surface elevation is composed of the summation of the depth y and the elevation z at the channel bottom above a datum, i.e.,

$$h = y + z \quad (2.41)$$

then:

$$\frac{\partial h}{\partial x} = \frac{\partial y}{\partial x} + \frac{\partial z}{\partial x} \quad (2.42)$$

However, since from Fig. 2.1 it is seen that:

$$S_o = - \frac{dz}{dx} = - \frac{\partial z}{\partial x} \quad (2.43)$$

Therefore, Equation (2.42) becomes:

$$\frac{\partial h}{\partial x} = \frac{\partial y}{\partial x} - S_o \quad (2.44)$$

The last term (the wind shear effect) may be expressed in a more convenient form by letting:

$$W_f = \frac{\tau_w}{\rho} = C_w |V_r \cos \omega| V_r \cos \omega \quad (2.45)$$

in which ω is the acute angle that the wind direction makes with the x-axis of the channel, C_w is a non-dimensional wind coefficient which can assume values ranging from 1.0×10^{-6} to 3.0×10^{-6} , and V_r is the relative velocity of the wind in relation to the velocity V of the fluid in the control volume, i.e.,

$$V_r = \pm V_w + V \quad (2.46)$$

where V_w is the velocity of the wind at approximately 9 ft above the free surface and the sign is (+) if opposing the velocity of the water and (-) if aiding the flow.

After substituting Equations (2.44) and (2.45) and $V = Q/A$ in Equation (2.40), the following is obtained:

$$\frac{\partial Q}{\partial t} + \frac{\partial(\beta Q^2/A)}{\partial x} + g A \left(\frac{\partial h}{\partial x} + S_f \right) - \beta q v_x + W_f B = 0 \quad (2.47)$$

An eddy loss term S_e similar to the friction slope S_f can be added to Equation (2.47) to account for head losses in addition to those due to boundary friction. These losses are due to large scale eddies formed in the flow at rather abrupt changes in the cross-section along the channel x-axis. The eddy loss slope S_e is evaluated using the following empirical equation:

$$S_e = \frac{K_e (\Delta V^2)}{2g (\Delta x)} \quad (2.48)$$

in which K_e is a non-dimensional coefficient of contraction and expansion, positive if contraction and negative if expansion.

After including the eddy loss term in Equation (2.47), the following is obtained:

$$\frac{\partial Q}{\partial t} + \frac{\partial(\beta Q^2/A)}{\partial x} + gA\left(\frac{\partial h}{\partial x} + S_f + S_e\right) - \beta q v_x + W_f B = 0 \quad (2.49)$$

This is the conservation form of the equation of motion that will be used herein.

Sometimes a different form of Equation (2.49) is required for certain finite difference schemes. If β is taken as unity and making use of $Q = AV$, Equation (2.49) can be expanded to give:

$$\begin{aligned} A \frac{\partial V}{\partial t} + V \frac{\partial A}{\partial t} + 2 \frac{Q}{A} \frac{\partial Q}{\partial x} - \frac{Q^2}{A^2} \frac{\partial A}{\partial x} + gA\left(\frac{\partial h}{\partial x} + S_f + S_e\right) - q v_x \\ + W_f B = 0 \end{aligned} \quad (2.50)$$

Then, substituting Equation (2.6) for $\partial A/\partial t$ and simplifying, the following is obtained:

$$\frac{\partial V}{\partial t} + V \frac{\partial V}{\partial x} + g\left(\frac{\partial h}{\partial x} + S_f + S_e\right) + \frac{q}{A} (V - v_x) + \frac{W_f B}{A} = 0 \quad (2.51)$$

and making use of Equation (2.44) yields:

$$\frac{\partial V}{\partial t} + V \frac{\partial V}{\partial x} + g\left(\frac{\partial y}{\partial x} - S_o + S_f + S_e\right) + \frac{q}{A} (V - v_x) + \frac{W_f B}{A} = 0 \quad (2.52)$$

The Saint-Venant Equations

The original Saint-Venant equations, first published by Barré de Saint-Venant [1871], did not include lateral inflow, wind effect, or eddy loss. Neglecting these terms in Equations (2.6) and (2.51) and using $Q = AV$, they become the original Saint-Venant equations, i.e.,

$$\frac{\partial(AV)}{\partial x} + \frac{\partial A}{\partial t} = 0 \quad (2.53)$$

$$\frac{\partial V}{\partial t} + V \frac{\partial V}{\partial x} + g\left(\frac{\partial h}{\partial x} + S_f\right) = 0 \quad (2.54)$$

The original Saint-Venant equations are expressed in terms of the unknowns V and h , while the conservation form of the Saint-Venant equations with lateral inflow and wind are expressed in terms of the unknowns Q and h . The conservation forms, Equations (2.7) and (2.49), are repeated here for convenient reference:

$$\frac{\partial Q}{\partial x} + \frac{\partial (A+A_o)}{\partial t} - q = 0 \quad (2.55)$$

$$\frac{\partial Q}{\partial t} + \frac{\partial (\beta Q^2/A)}{\partial x} + gA \left(\frac{\partial h}{\partial x} + S_f + S_e \right) - \beta q v_x + W_f B = 0 \quad (2.56)$$

The terms in Equations (2.53)-(2.56) are defined as: x = longitudinal distance along the channel, positive in the downstream direction; t = time; A = cross-sectional area of flow; A_o = off-channel dead storage; V = mean velocity of flow across a section, positive in the downstream direction; h = water surface elevation; q = known lateral inflow or outflow per unit length along the channel, positive if inflow; v_x = velocity of lateral flow in the direction of the channel flow; S_f = friction slope; S_e = eddy loss slope; B = top width of channel at water surface; W_f = wind resistance effect; β = momentum correction factor; and g = acceleration due to gravity.

The friction slope S_f can be evaluated by an empirical resistance equation such as the Manning equation, i.e.,

$$S_f = \frac{n^2 |Q|Q}{2.21 A^2 R^{4/3}} \quad (2.57)$$

in which n is the Manning roughness coefficient. The absolute value of Q is used so that the algebraic sign of the friction slope will be the same as that associated with Q . In this way, momentum conservation is properly represented for negative flow, i.e., flow proceeding in the upstream direction. The hydraulic radius which is defined as A/P can be adequately approximated by the hydraulic depth A/B for most natural river channels for which $B > 10 y$.

The eddy loss slope S_e is evaluated using Equation (2.48) repeated here for convenience:

$$S_e = \frac{K_e (\Delta V^2)}{2g (\Delta x)} \quad (2.58)$$

in which K_e is a dimensionless coefficient. Cross-sections contracting abruptly in the direction of flow have K_e values ranging from 0 to 0.4, while abruptly expanding cross-sections have negative K_e values ranging from 0.5 to unity. The larger coefficients are associated with the more abrupt contractions and expansions of the cross-section.

The wind effect W_f can be evaluated using Equation (2.45) repeated here for convenience:

$$W_f = C_w |V_r \cos \omega| V_r \cos \omega \quad (2.59)$$

in which C_w is the wind coefficient, ω is the acute angle that the wind makes with the x -axis, and V_r is the relative velocity of the wind and the flow as given by Equation (2.46). The absolute value of $V_r \cos \omega$ is used for a similar reason as in Equation (2.57).

The momentum correction factor β is usually assumed to be unity, although it may be somewhat arbitrarily assigned values up to 1.3 if the velocity distribution in the cross-section is suspected to be distorted.

The lateral inflow q is a known function of time t and distance x along the channel axis. It has dimensions of ft^3/sec per linear ft of channel, i.e., ft^2/sec . If the lateral flow is into the channel, q is known as lateral inflow and has a positive algebraic sign associated with it. If the lateral flow is leaving the channel, q is known as lateral outflow and has a negative algebraic sign. However, in either case, the negative sign preceding the term q in Equations (2.55) and (2.56) does not change.

The cross-sectional area A and the top width B of the cross-section can be expressed as known functions of depth y or water surface elevation h , e.g.,

$$A = A(h) \quad (2.60)$$

$$B = B(h) \quad (2.61)$$

The functions may be simple algebraic relations for cross-sections of regular geometric shapes such as rectangles, triangles, trapezoids, or parabolic and circular shapes. For natural channels with irregularly shaped cross-sectional areas, the function may be a polynomial, e.g.,

$$B = a_1 h^3 + a_2 h^2 + a_3 h + a_4 \quad (2.62)$$

or the function may be a power type, e.g.,

$$B = a_1 h^{a_2} \quad (2.63)$$

Probably the most accurate as well as the easiest function to develop for irregularly shaped cross sections is a step-wise linear function. Whereas the polynomial and power type have advantages for certain analytical solutions of simplified forms of the Saint-Venant equations and for their conciseness, most natural cross-sections are not accurately represented in this manner and special computations involving least-square analysis are required to evaluate the coefficients. Since computers are required to obtain solutions to the complete Saint-Venant equations via finite difference techniques, the advantages associated with the polynomial and power type expressions are not relevant. The step-wise linear functions can be described by tabular values of B and h with linear interpolation used for intermediate values. This is easily handled by the computer with a high degree

of accuracy and requires a minimum of effort on the part of the user in preparing the tabular input. The step-wise linear representation of A and B will be described in detail in a later section. Actually only A or B need be specified since one can be derived from the other, e.g.,

$$B = dA/dh \quad (2.64)$$

or:

$$A = \int_0^h B \, dh \quad (2.65)$$

The first term in the continuity equation (2.55) is the rate of change of discharge along the x-axis. If this term were multiplied by $dx \, dt$, it would have dimensions of volume. This volume represents the so-called wedge and prism storages associated with well-known storage flood routing methods. The second term is the rate of change of cross-sectional area with time. If it were multiplied by $dx \, dt$, it would have dimensions of volume. This volume represents the positive or negative storage of water along the channel due to the change in water surface elevation over an interval of time. The third term is the lateral inflow. Again, if it were multiplied by $dx \, dt$, it would have dimensions of volume representing the positive or negative storage of water due to the lateral inflow or outflow.

The terms in the momentum equation (2.56) have dimensions of ft^3/sec^2 . If the terms were divided by A, the resulting dimension would be ft/sec^2 , or an acceleration rate. The first term would represent the local (temporal) acceleration due to the rate of change of flow. The second term would represent the convective (spatial) acceleration or the so-called Bernoulli effect due to the change in flow along the x-axis. The third term would be the acceleration due to the combined effects of gravity, unbalanced pressure head, and channel boundary friction and eddy losses. The fourth term would represent the acceleration contributed by the lateral inflow in the direction of the x-axis. The last term would represent the acceleration due to frictional effects of wind at the free surface of the flow.

The conservation equations (2.55) and (2.56) or the non-conservation equations (2.53) and (2.54) constitute a system of first-order quasi-linear (non-linear) partial differential equations of the hyperbolic type. They have x and t as independent variables and h and Q or V as dependent variables. The other terms are constants or are functions of independent or dependent variables, i.e., $A(x,h)$, $B(x,h)$, $R(A,B)$, $n(x,h \text{ or } Q)$, $q(x,t)$, $v_x(x,t)$, $W_f(x,t)$. The non-linearity arises from the presence of Q in the second term of Equation (2.56) and also in Equation (2.57). Non-linearity is also introduced through A^2 and $R^{4/3}$ in Equation (2.57). Also, if A is a non-linear function of h, this contributes to the non-linearity of the equations. The term

$V \partial V / \partial x$ also adds to the non-linearity of Equation (2.54). The classification of the equations as hyperbolic differentiates the similarity of the mathematical properties of this type of equation from those associated with groups of partial differential equations known as parabolic and elliptic equations. The hyperbolic type is characterized by having two real and distinct characteristic directions or curves on an x - t plane representing the solution domain of the equations. Along these curves the partial differential equations reduce to equations involving total differentials only. This feature gives rise to the so-called "method of characteristics," which can be used to solve the Saint-Venant equations and is presented briefly in a later section. The parabolic type of equations have two real and equal characteristic directions while the elliptic have two distinct but imaginary characteristic directions.

The Saint-Venant equations have no analytical solutions except for cases where the channel geometry is uniform and the non-linear properties of the equations are neglected or linearized. However, the complete Saint-Venant equations can be approximated by finite difference expressions and the resulting algebraic difference equations numerically integrated via digital computers to obtain solutions of V and h in the case of Equations (2.53) and (2.54) or Q and h for Equations (2.55) and (2.56) for discrete values of x and t .

The manner in which the finite differences are approximations of the partial differential equations may require some further clarification. Finite difference solution techniques for partial differential equations are approximate in the sense that derivatives at a point are approximated by difference quotients over a small interval, i.e., $\partial Q / \partial x$ is replaced by $\Delta Q / \Delta x$, where Δx is small, but the finite difference solutions are not approximate in the sense of being crude estimates. Data pertaining to the differential equations, e.g., A , h , and Q , are invariably subject to errors of measurement. Also, all arithmetical work is limited to a finite number of significant figures and contain round-off errors, so that even analytical solutions provide only approximate answers. Finite difference methods generally give solutions that are either as accurate as the data warrants or as accurate as necessary for the purposes for which the solutions are required. In both cases, a finite difference solution is as satisfactory as one calculated from an analytical formula.

Some finite difference techniques will be briefly described in following sections. One particular finite difference scheme, known as the "weighted four-point implicit" scheme will be described in detail.

3. SOLUTION METHODS OF THE SAINT-VENANT EQUATIONS

Introduction

The complete Saint-Venant equations previously derived in section 2 constitute a system of non-linear hyperbolic partial differential equations. There are two fundamental classes of methods for solving these equations.

One class, known as the method of characteristics, converts the original system of partial differential equations to an equivalent system of ordinary differential equations. Then, finite difference approximations to the ordinary derivatives are introduced and solutions are then obtained from the resulting system of algebraic equations.

The second fundamental class of solution methods is known as finite difference methods. In these methods, finite difference approximations are substituted directly into the original system of partial differential equations. Depending on the particular finite difference approximation used, the method of solution is known as either explicit or implicit.

In this section, a brief description of each of the two classes of solution methods will be presented. First, the method of characteristics is presented. Then, the concept of finite differences is introduced. Finally, the method of finite differences consisting of explicit and implicit variations are presented.

Method of Characteristics

The method of characteristics has been used extensively to solve the Saint-Venant equations. Among the investigators who have used this method are: Amein [1966], Streeter and Wylie [1967], Fletcher and Hamilton [1967], Lai [1967], Liggett and Woolhiser [1967], Ellis [1970], Wylie [1970], and Fread and Harbaugh [1973a]. Although the method of characteristics is a powerful mathematical tool, it has some disadvantages when the Saint-Venant equations are applied to natural channels. For example, the addition of certain terms such as the off-channel storage term A_0 in Equation (2.6) requires a major change to the ordinary differential equations derived from the Saint-Venant equations not containing the off-channel storage term. Also, solutions to the characteristic form of the equations are not fixed in space or at specified intervals in time. This creates the need for interpolation schemes which add to the complexity of the solution procedure and introduce additional errors of approximation.

Development of characteristic equations

The non-conservative Saint-Venant equations for a prismatic channel with no lateral inflow were derived in the preceding section.

They are:

$$\frac{\partial y}{\partial t} + \frac{A}{B} \frac{\partial V}{\partial x} + v \frac{\partial y}{\partial x} = 0 \quad (3.1)$$

$$\frac{\partial V}{\partial t} + v \frac{\partial V}{\partial x} + g \frac{\partial y}{\partial x} + g (S_f - S_o) = 0 \quad (3.2)$$

This set of equations forms a system of hyperbolic partial differential equations in terms of two independent variables, x and t , and two dependent variables, V and y . A general analytic solution of this system has not been developed; however, a solution can be obtained by the "method of characteristics." In this method, the two partial differential equations are transformed into four unique total differential equations. The total differential equations can then be solved on a digital computer by either explicit or implicit finite-difference numerical integration techniques.

In developing the total differential equations, i.e., "characteristic equations," Equations (3.1) and (3.2) are combined into a single partial differential equation [Streeter and Wylie, 1967; Fread and Harbaugh [1971a]. However, in order to combine the two equations, their dimensions must be identical. Upon examining the dimensions of each equation, it is seen that the dimensions of Equation (3.1) are ft/sec while those of Equation (3.2) are ft/sec². Therefore, before forming the combination, Equation (3.2) must be multiplied by an unknown multiplier ψ having the necessary dimensions to transform the dimensions of Equation (3.2) to those of Equation (3.1). Then a combination may be formed by simply adding Equations (3.1) and (3.2). Thus:

$$\frac{\partial y}{\partial t} + \frac{A}{B} \frac{\partial V}{\partial x} + v \frac{\partial y}{\partial x} + \psi \left(\frac{\partial V}{\partial t} + v \frac{\partial V}{\partial x} + g \frac{\partial y}{\partial x} + g (S_f - S_o) \right) = 0 \quad (3.3)$$

Rearranging Equation (3.3) such that the partial derivatives of V and y are grouped together, respectively, one obtains:

$$\psi \left(\frac{\partial V}{\partial t} + \left(v + \frac{A}{\psi B} \right) \frac{\partial V}{\partial x} \right) + \left(\frac{\partial y}{\partial t} + (v + \psi g) \frac{\partial y}{\partial x} \right) + \psi g (S_f - S_o) = 0 \quad (3.4)$$

Now, the identity of the unknown multiplier ψ is not known, but it is known that the characteristic equations being sought will contain derivatives of V and y in a particular direction only. Thus, the derivatives to be

obtained will be total derivatives rather than partial derivatives, as shown by Equations (3.5) and (3.6).

$$\frac{dV}{dt} = \frac{\partial V}{\partial t} + \frac{dx}{dt} \frac{\partial V}{\partial x} \quad (3.5)$$

and

$$\frac{dy}{dt} = \frac{\partial y}{\partial t} + \frac{dx}{dt} \frac{\partial y}{\partial x} \quad (3.6)$$

The direction along which these derivatives are formed is known as the "characteristic direction."

It is apparent that the bracketed quantities in Equation (3.4) are total derivatives, where dx/dt takes on the values:

$$\frac{dx}{dt} = v + \frac{A}{\psi B} \quad (3.7)$$

and

$$\frac{dx}{dt} = v + \psi g \quad (3.8)$$

Since the right-hand sides of Equations (3.7) and (3.8) are equal to the same quantity, dx/dt , then:

$$v + \frac{A}{\psi B} = v + \psi g \quad (3.9)$$

or

$$\psi^2 = \frac{A}{gB} \quad (3.10)$$

Thus, the multiplier ψ is found to be:

$$\psi = \pm \sqrt{\frac{A}{gB}} \quad (3.11)$$

where ψ has dimensions of sec.

Substituting this expression for ψ into either Equation (3.8) or (3.9) results in:

$$\frac{dx}{dt} = v \pm \sqrt{gA/B} \quad (3.12)$$

The term dx/dt represents the inverse slope of every point on a curve C in an x-t coordinate system. The curve C is called the characteristic direction of the partial differential Equation (3.5). Depending upon the sign before the radical in Equation (3.12), there are two inverse slopes, dx/dt . This signifies that two characteristic curves exist, along which the partial derivatives of Equation (3.5) are total derivatives. The two directions are defined as a positive characteristic direction C+ and a negative characteristic direction C- as shown in Fig. 3.1.

The differential equation of the C+ curve is:

$$\frac{dx}{dt} = v + \sqrt{gA/B} \quad (3.13)$$

and that for the C- curve is:

$$\frac{dx}{dt} = v - \sqrt{gA/B} \quad (3.14)$$

The term dx/dt , as given by Equations (3.13) and (3.14), allows the bracketed quantities in Equation (3.5) to be written as total derivatives of V and y; thus, Equation (3.5) reduces to:

$$\psi \frac{dV}{dt} + \frac{dy}{dt} + \psi g (S_f - S_o) = 0 \quad (3.15)$$

Equations (3.1) and (3.2) or their linear combination, Equation (3.5), are generally referred to as quasi-linear, hyperbolic, partial differential equations. They are quasi-linear since all derivatives are first order. The equations are hyperbolic since the characteristic directions, as given by Equations (3.13) and (3.14), are real and distinct. Substituting the two values of ψ into Equation (3.15), one obtains the following two equations:

$$\frac{dV}{dt} + \sqrt{gB/A} \frac{dy}{dt} + g (S_f - S_o) = 0 \quad (3.16)$$

and

$$\frac{dV}{dt} - \sqrt{gB/A} \frac{dy}{dt} + g (S_f - S_o) = 0 \quad (3.17)$$

Equation (3.16) is valid along the C+ direction described by Equation (3.13), and Equation (3.17) is valid for the C- direction described by Equation (3.14). These equations form the system of equations which contain the four Characteristic Equations whose derivatives are composed of total derivatives, rather than partial derivatives. Thus:

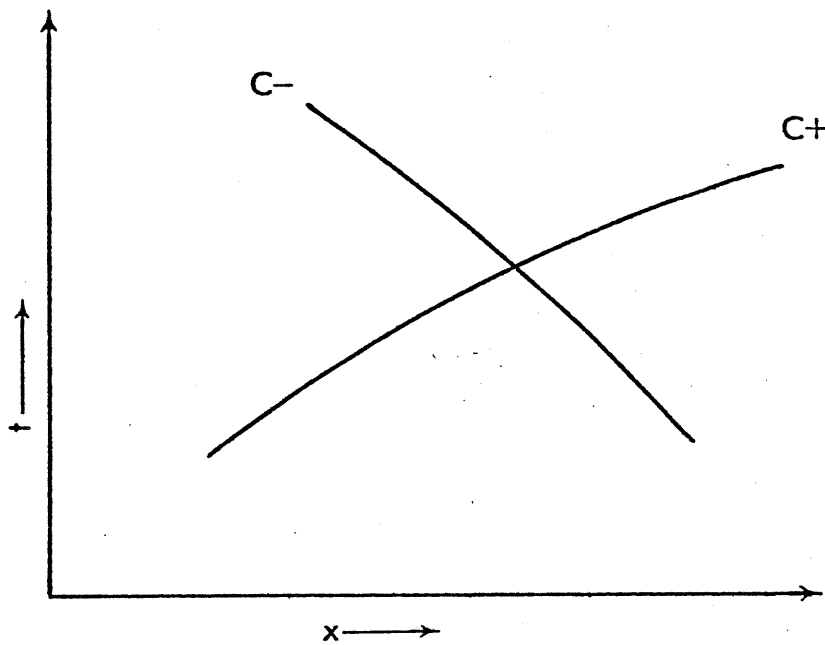


Fig. 3.1.—Characteristic curves in the x - t plane.

$$\left. \begin{aligned} \frac{dV}{dt} + \sqrt{gB/A} \frac{dy}{dt} + g (S_f - S_o) &= 0 \\ \frac{dx}{dt} &= V + \sqrt{gA/B} \end{aligned} \right\} \begin{array}{l} C+ \\ \\ \end{array} \quad (3.18)$$

$$\left. \begin{aligned} \frac{dV}{dt} - \sqrt{gB/A} \frac{dy}{dt} + g (S_f - S_o) &= 0 \\ \frac{dx}{dt} &= V - \sqrt{gA/B} \end{aligned} \right\} \begin{array}{l} C- \\ \\ \end{array} \quad (3.19)$$

First-order finite-difference approximation

The Characteristic Equations, (3.18) and (3.19), do not possess an exact analytic solution; however, they may be solved by a first-order explicit finite-difference approximation technique. The C+ and C- curves, defined by Equations (3.18) and (3.19), describe a curvilinear net in an x-t coordinate system or x-t plane, as shown in Fig. 3.2.

Denote P as the point of intersection of the C+ characteristic passing through point L and of the C- characteristic passing through point R. (Note that P exists if points L and R are sufficiently close together since $C+ \neq C-$.) Now, for notational purposes, let x_L represent the value of x at point L, t_L represent the value of t at point L, etc. Likewise, x_R , t_R , V_R , and y_R represent the values of x, t, V, and y at point R; and x_P , t_P , V_P , and y_P represent the values of x, t, V, and y at point P.

The Characteristic Equations, (3.18) and (3.19), may now be represented by the following general first-order (linear) finite-difference approximation in the form:

$$\int_{x_0}^{x_1} f(x) dx \approx f(x_0)(x_1 - x_0) \quad (3.20)$$

The total derivatives of Equations (3.18) are replaced by the following finite-difference quotients:

$$\frac{dV}{dt} \approx \frac{V_P - V_L}{t_P - t_L}, \quad \frac{dy}{dt} \approx \frac{y_P - y_L}{t_P - t_L}, \quad \text{and} \quad \frac{dx}{dt} \approx \frac{x_P - x_L}{t_P - t_L} \quad (3.21)$$

and the total derivatives of Equations (3.19) are replaced by:

$$\frac{dV}{dt} \approx \frac{V_P - V_R}{t_P - t_R}, \quad \frac{dy}{dt} \approx \frac{y_P - y_R}{t_P - t_R}, \quad \text{and} \quad \frac{dx}{dt} \approx \frac{x_P - x_R}{t_P - t_R} \quad (3.22)$$

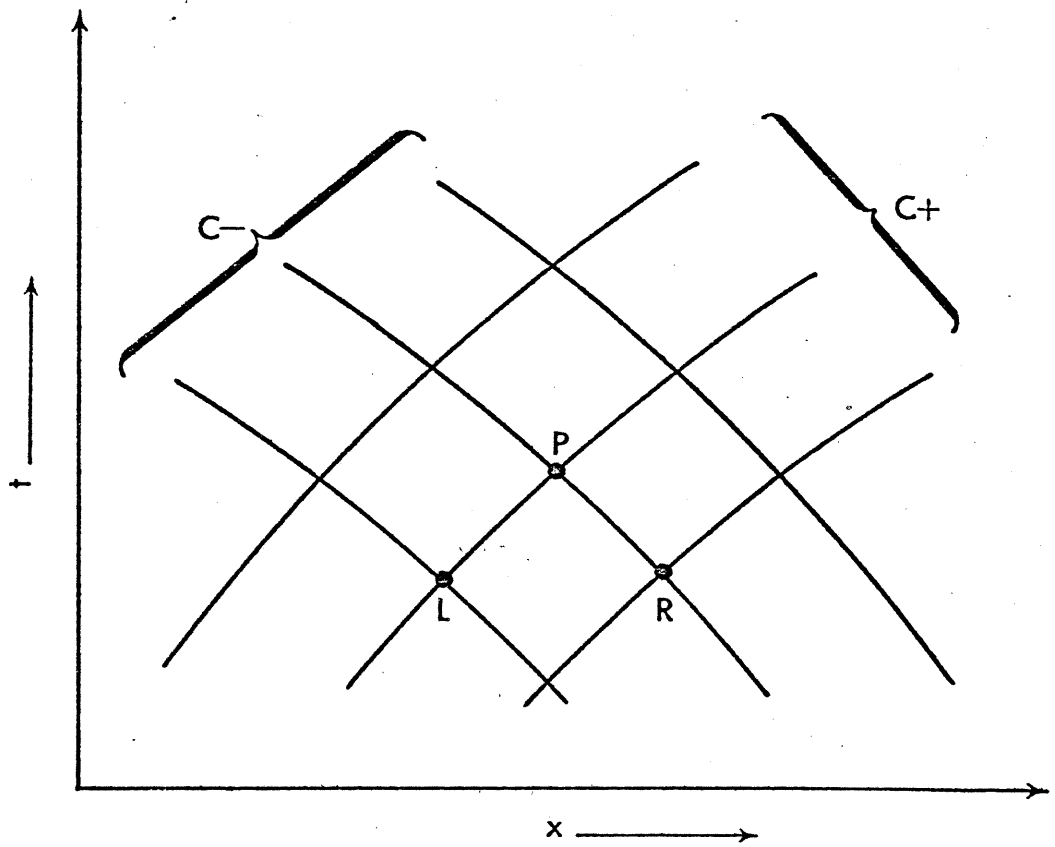


Fig. 3.2.—Characteristic net in x - t plane.

Upon substituting the above approximations for the total derivatives, applying the definition of a first-order finite-difference approximation (3.20) for a differential equation, and dividing through by the finite-difference expression for dt, Equations (3.18) and (3.19) become, respectively:

$$\left. \begin{aligned} V_P - V_L + \sqrt{gB_L/A_L} (y_P - y_L) + (t_P - t_L) g (S_{f_L} - S_o) &= 0 \\ x_P - x_L &= (V_L + \sqrt{gA_L/B_L}) (t_P - t_L) \end{aligned} \right\} \text{C+ (3.23)}$$

$$\left. \begin{aligned} V_P - V_R - \sqrt{gB_R/A_R} (y_P - y_R) + (t_P - t_R) g (S_{f_R} - S_o) &= 0 \\ x_P - x_R &= (V_R - \sqrt{gA_R/B_R}) (t_P - t_R) \end{aligned} \right\} \text{C- (3.24)}$$

Thus, if x_L , t_L , V_L , y_L , x_R , t_R , V_R , and y_R are known values, the solution for x_P , t_P , V_P , and y_P can be obtained. In this way, a solution can proceed from time line to time line in Δt increments of time.

Computation of interior points

Equations (3.23) and (3.24) form a system of equations, each of which are linear with respect to the unknown variables x_P , t_P , V_P , and y_P . This linear system of four equations and four unknowns may be readily solved for the unknown variables in the following manner. The second of Equations (3.24) is subtracted from the second of Equations (3.23), and the following expression for t_P is obtained:

$$t_P = \frac{[x_L - x_R + t_R (V_R - \sqrt{gA_R/B_R}) - t_L (V_L + \sqrt{gA_L/B_L})]}{(V_R - V_L - \sqrt{gA_L/B_L} - \sqrt{gA_R/B_R})} \quad (3.25)$$

Since the value of t_P has been found, x_P may be obtained directly from the second of Equations (3.23), which results in:

$$x_P = x_L + (V_L + \sqrt{gA_L/B_L}) (t_P - t_L) \quad (3.26)$$

The first of Equations (3.24) is then subtracted from the first of Equations (3.23), and the following expression for y_P is obtained:

$$\begin{aligned} y_P &= [V_L - V_R + \sqrt{gB_L/A_L} y_L + \sqrt{gB_R/A_R} y_R - (t_P - t_L) g (S_{f_L} - S_o) \\ &+ (t_P - t_R) g (S_{f_R} - S_o)] / (\sqrt{gB_L/A_L} + \sqrt{gB_R/A_R}) \end{aligned} \quad (3.27)$$

Since the values of y_p and t_p have been found, V_p may be obtained directly from the first of Equations (3.23), i.e.,

$$V_p = V_L - \sqrt{gB_L/A_L} (y_p - y_L) - (t_p - t_L) g(S_{f_L} - S_o) \quad (3.28)$$

It should be noted that each point in the $x-t$ plane has a "domain of dependence" and conversely a "range of influence." Referring to Fig. 3.3, the values of V and y at point T are dependent upon the values of V and y at all points within the shaded curvilinear region of the $x-t$ plane, i.e., the domain of dependence of point T is the shaded region.

In Fig. 3.4, the values of V and y at point M will affect the values of V and y at all points within the shaded curvilinear region of the $x-t$ plane, i.e., the range of influence of point M is the shaded region.

By applying Equations (3.25) through (3.28), the values of x , t , V , and y may be determined for all points lying interior to the $x-t$ plane. Each computed point will be dependent upon previously computed points and will in turn influence successively computed points.

Initial conditions

An initial condition must be known if solutions to an unsteady flow problem are to be obtained. The term "initial condition" refers to the state of the flow within the channel reach prior to the time at which solutions of the unsteady flow equations are sought, i.e., at time $t=0$ on the $x-t$ plane. In Fig. 3.5, the initial condition pertains to the values of x , t , V , and y for points I_1 , I_2 , I_3 , I_4 , and I_5 . Usually, the points are evenly spaced along the channel reach.

Boundary conditions

Boundary conditions are necessary for a complete solution to an unsteady flow problem and, indeed, the boundary condition usually describes the unsteady disturbance to which the channel reach is subjected. Boundary conditions refer to known relationships which exist between the unknown variables x , t , V , or y at each end of the channel reach. These relationships are independent of the unsteady flow equations, and they must be valid throughout the interval of time for which solutions to the unsteady flow equations are sought.

Referring to Fig. 3.5, the points U , U_1 , and U_2 in the $x-t$ plane are upstream boundary points and D , D_1 , and D_2 are downstream boundary points. The C^- Characteristic Equations (3.24) are used for computing the unknown variable associated with the upstream boundary points, and the C^+ Characteristic Equations (3.23) are used for computing the unknown variables associated with downstream boundary points. If boundary points are not prescribed for an unsteady flow problem, the unknown

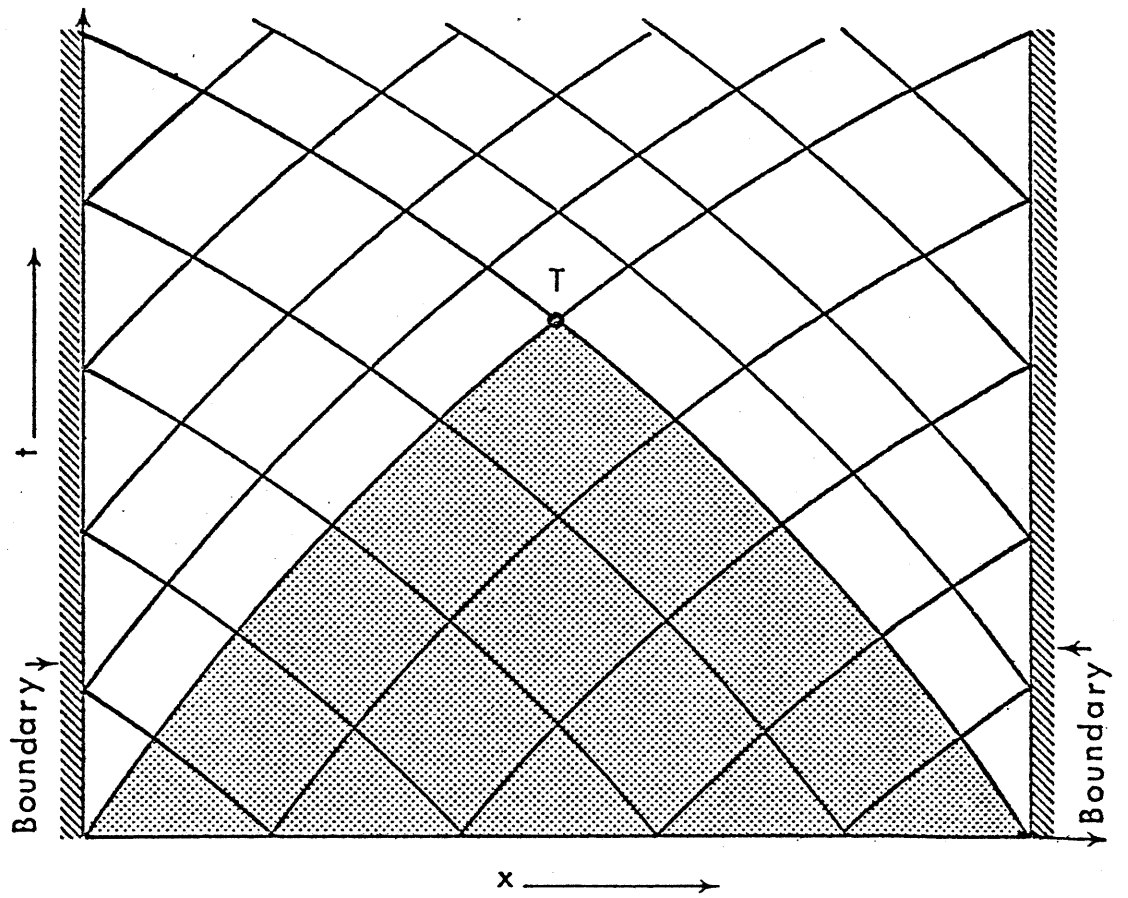


Fig. 3.3.—Domain of dependence for point T.

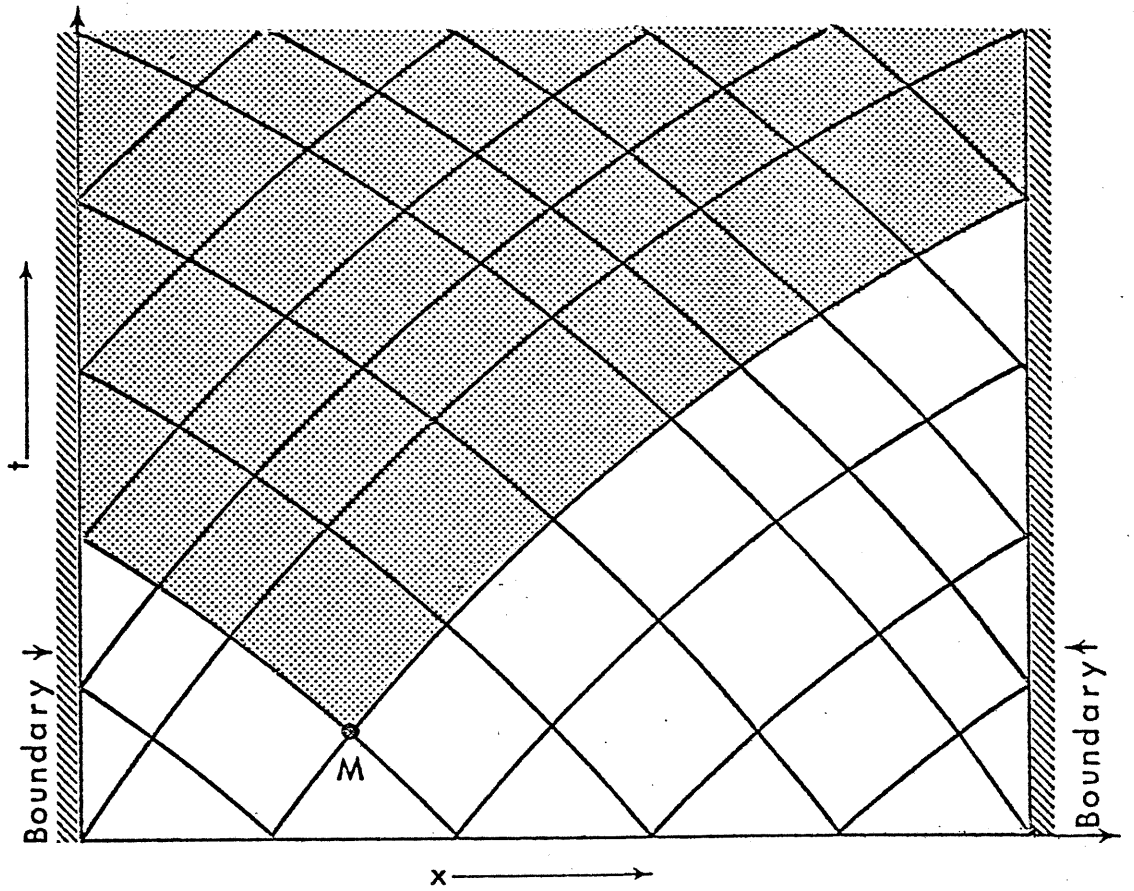


Fig. 3.4.--Range of influence of point M.

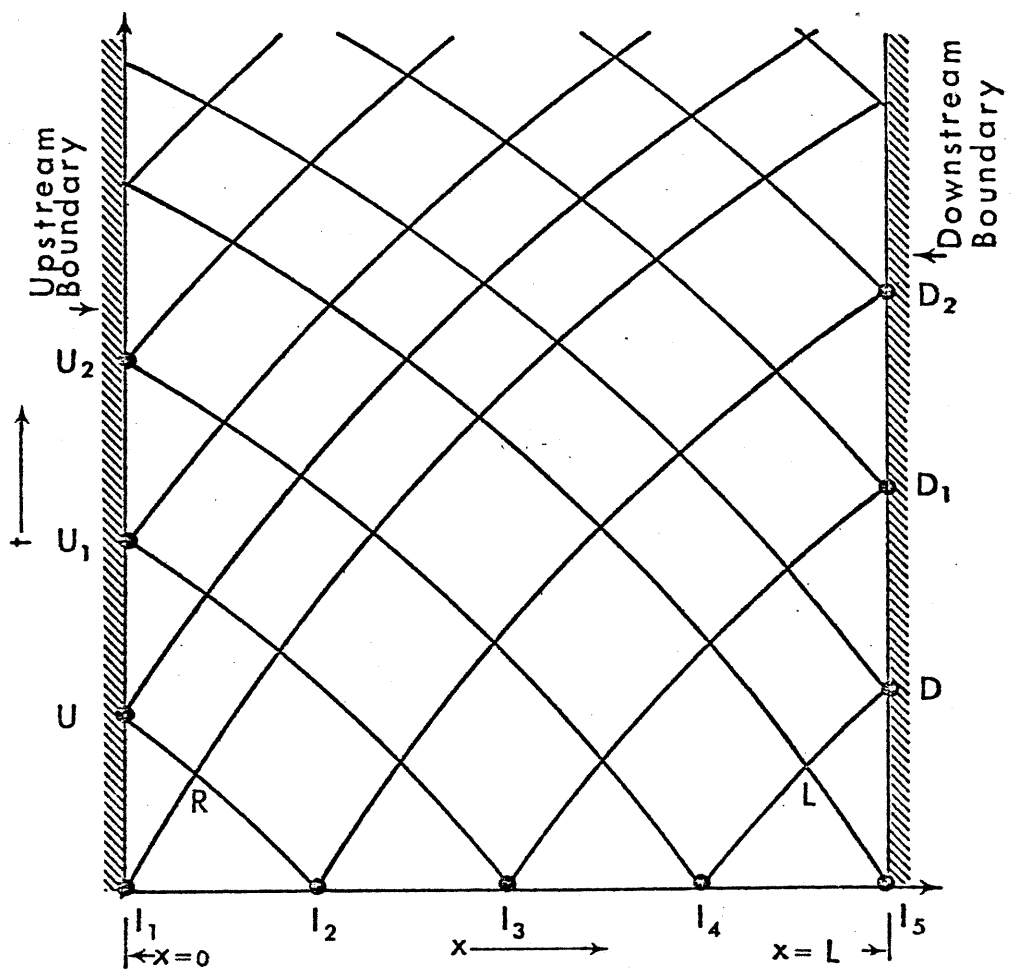


Fig. 3.5.—Characteristic net with initial points.

variables x , t , y and V associated with the points within and on the shaded region of Fig. 3.5 are the only ones which can be computed from the unsteady flow equations. Of course, this assumes that the initial condition (points along the $t=0$ axis of the $x-t$ plane) has been specified.

The following examples are boundary conditions which might be prescribed:

1. Upstream discharge hydrograph: A common upstream boundary is a discharge hydrograph. In this condition, the discharge entering the channel reach is known as a function of time, i.e., $Q = Q(t)$. Thus, from continuity considerations, the independent relationship at the upstream boundary is given by:

$$Q = A(t) V(t) \quad (3.29)$$

Referring to Fig. 3.5, it is assumed that the values of x , t , V , and y at point R are known and it is desired to find the values of x , t , V , and y at the upstream boundary point U. The C-Characteristic Equations (3.24), where the subscript P is replaced by U, are applicable to an upstream boundary point. Upon examining Equations (3.24), it is seen that x_U is known, i.e., $x_U = 0$; thus, t_U may be computed directly from the second of Equations (3.24), resulting in:

$$t_U = t_R - x_R / (V_R - \sqrt{gA_R/B_R}) \quad (3.30)$$

From Equation (3.29), $V_U = Q/A_U$ and the first of Equations (3.24) becomes:

$$Q/A_U - \sqrt{gB_R/A_R} y_U - V_R + \sqrt{gB_R/A_R} y_R + (t_U - t_R) g(S_{f_R} - S_o) = 0 \quad (3.31)$$

This equation is non-linear with respect to the unknown y_U due to the presence of the term A_U . An iterative solution technique such as the Newton-Raphson method can be used to solve Equation (3.31) for y_U . The Newton-Raphson method is presented in Appendix A.

2. Upstream stage hydrograph: In this case, $y = y(t)$, i.e., y_U is known at any time t . Since $x_U = 0$ and t_U may be computed from Equation (3.30), V_U may be directly computed from the first of Equations (3.28), i.e.;

$$V_U = V_R + \sqrt{gB_R/A_R} (y_U - y_R) - (t_U - t_R) g(S_{f_R} - S_o) \quad (3.32)$$

3. Normal flow at the downstream boundary: This downstream boundary condition is encountered when the channel is very long, in fact, long enough such that the effects of any unsteady disturbance at the upstream end of the channel have dissipated along the channel and are not noticed

at the downstream section. The flow at this boundary is subject to the restraints of normal flow as given by Manning's Equation (2.14) in which the friction slope S_f is assumed to be adequately defined by the channel bottom slope S_o , i.e.,

$$V = \frac{1.486}{n} S_o^{1/2} R^{2/3} \quad (3.33)$$

Referring to Fig. 3.3, it is assumed that the values of x , t , V , and y at point L are known, and it is desired to find these values associated with the downstream boundary point D. The C+ Characteristic Equations (3.23), where the subscript P is replaced by D, are applicable for computing downstream boundary points. Upon examining Equations (3.23), it is seen that x_D is known since it is the location of the downstream boundary, and t_D may be computed directly from the second of Equations (3.23), i.e.,

$$t_D = t_L + (x_D - x_L) / (V_L + \sqrt{gA_L/B_L}) \quad (3.34)$$

From Mannings equation (3.33):

$$V_D = \frac{1.486}{n} S_o^{1/2} R_D^{2/3} \quad (3.35)$$

Then, the first of Equations (3.23) becomes:

$$\begin{aligned} \frac{1.486}{n} S_o^{1/2} R_D^{2/3} + \sqrt{gB_L/A_L} y_D - V_L - \sqrt{gB_L/A_L} y_L \\ + (t_D - t_L) g(S_{f_L} - S_o) = 0 \end{aligned} \quad (3.36)$$

This equation is non-linear with respect to the unknown y_D due to the presence of the term R_D . The Newton-Raphson iterative method can be used to solve Equation (3.36) for y_D . Equation (3.35) is used to obtain V_D .

Finite Difference Approximations

The mathematical basis for finite difference approximations can be derived from a Taylor series expansion. Consider the function $U(x)$ in which the dependent variable U is a known function of the independent variable x as shown in Fig. 3.6. Its value at point P, i.e., x , is $U(x)$. The value of the function U at point Q, $x + \Delta x$, can be evaluated by the Taylor series expansion about x , i.e.,

$$U(x+\Delta x) = U(x) + \Delta x U'(x) + \frac{1}{2} \Delta x^2 U''(x) + \frac{1}{6} \Delta x^3 U'''(x) + \dots (3.37)$$

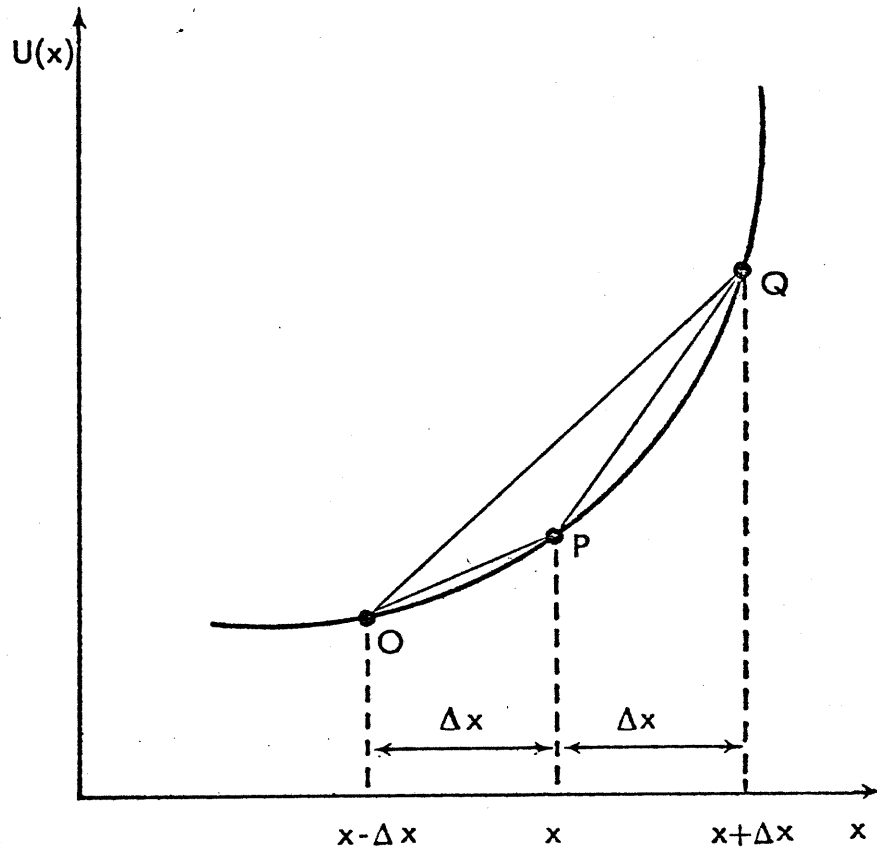


Fig. 3.6.--Derivation of finite difference approximations for derivatives.

and its value at point 0, $x - \Delta x$, is:

$$U(x-\Delta x) = U(x) - \Delta x U'(x) + \frac{1}{2} \Delta x^2 U''(x) - \frac{1}{6} \Delta x^3 U'''(x) + \dots \quad (3.38)$$

in which $U'(x)$, $U''(x)$, and $U'''(x)$ denote respectively, first, second, and third derivatives of the function U at point x , i.e., at point P in Fig. 4.1. Subtraction of these expansions gives:

$$U(x + \Delta x) - U(x - \Delta x) = 2\Delta x U'(x) + O(\Delta x^3) \quad (3.39)$$

where $O(\Delta x^3)$ denotes terms containing third and higher powers of Δx . Assuming these are negligible in comparison with lower powers of Δx , it follows that:

$$U'(x) \approx \frac{U(x+\Delta x) - U(x-\Delta x)}{2\Delta x} \quad (3.40)$$

i.e.,

$$U'_P \approx \frac{U_Q - U_0}{2\Delta x} \quad (3.41)$$

with an error of approximation (truncation error) of order Δx^2 . Referring to Fig. 3.1, it is seen that Equation (3.41) clearly approximates the slope of the tangent at P by the slope of the chord OQ . Equation (3.41) is known as a central-difference approximation.

If the function $U(x)$ is subtracted from Equation (3.37), a forward-difference approximation is obtained, i.e.,

$$U(x + \Delta x) - U(x) = \Delta x U'(x) + O(\Delta x^2) \quad (3.42)$$

Thus:

$$U'(x) \approx \frac{U(x+\Delta x) - U(x)}{\Delta x} \quad (3.43)$$

i.e.,

$$U'_P \approx \frac{U_Q - U_P}{\Delta x} \quad (3.44)$$

with an error of approximation of order Δx . In Fig. 3.6, it is evident that the slope of the tangent at P is approximated by Equation (3.44) as the slope of the chord PQ .

Similarly, the expression for a backward-difference approximation is obtained by subtracting Equation (3.38) from $U(x)$, i.e.,

$$U(x) - U(x - \Delta x) = \Delta x U'(x) + O(\Delta x^2) \quad (3.45)$$

Thus:

$$U'(x) \approx \frac{U(x) - U(x-\Delta x)}{\Delta x} \quad (3.46)$$

i.e.,

$$U'_P \approx \frac{U_P - U_0}{\Delta x} \quad (3.47)$$

with an error of approximation of order Δx . In Fig. 3.6, this is seen to be an approximation of the slope of the tangent at P using the slope of the chord OP.

In the application of the method of finite differences to the Saint-Venant equations, the concept is first introduced of a so-called "x-t" plane. As shown in Fig. 3.7, the x-t plane consisting of a rectangular net of discrete points represents the continuous solution domain defined by the independent variables (x and t) in the Saint-Venant equations. The net points are defined by the intersection of straight lines drawn parallel to the axes of the x-t plane. Lines parallel to the x-axis are "time lines" and have a spacing of Δt called the "time step." Each discrete point in the x-t plane is identified by a subscript (i) which designates the x-position and a superscript (j) which designates the time line. The time and/or the distance steps must be equal in certain finite difference schemes while in others they do not have to be equal.

Since the finite differences are only approximations to the original partial differential equations, it is important that the error of approximation be minimal. The error of approximation (truncation or discretization error) arises from the omission of higher order terms in deriving the finite difference expressions such as Equations (3.41), (3.44), and (3.47). The condition where the truncation error approaches zero as Δx and Δt approach zero is known as "consistency." Closely related to the consistency of the finite difference scheme is the property known as "convergence," which is the condition in which the solution of the finite difference approximation of the original partial differential equation approaches the analytical solution of the differential equation.

Another property of finite difference schemes is the so-called "numerical stability." A scheme is numerically stable if numerical errors introduced in the computations such as round-off of irrational numbers are not amplified during successive computations such as to entirely mask the true solution. Numerical instability is characterized by expanding oscillations of the solutions of the dependent variables (depth and velocity or discharge) with successive time steps.

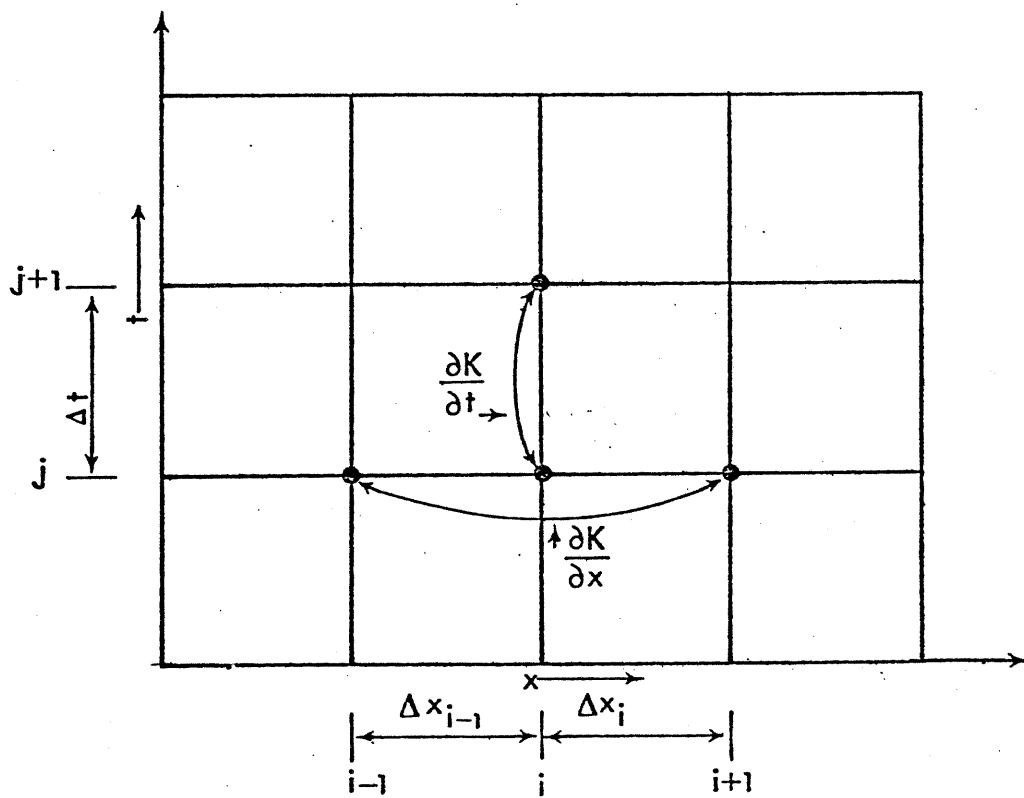


Fig. 3.7.—Finite difference approximations for explicit diffusion scheme.

Explicit Finite Difference Methods

The term explicit refers to those finite difference methods (schemes) that advance the solution of the Saint-Venant equations point by point along one time line until all the unknowns associated with that time line have been evaluated. Then, the solution is advanced to the next time line in the x-t plane. In an explicit scheme, the spatial derivatives and non-derivative terms are evaluated on the time line t^j where the values of all variables are known. Only the time derivatives contain unknowns. Thus, in an explicit method, two linear algebraic equations are generated from the two Saint-Venant equations at each net point (node). Since the two equations can be solved directly for the unknowns, the equations are described as "explicit."

The development of explicit methods resulted from the pioneering work of Stoker [1953] and Isaacson *et al.* [1954, 1956, 1958] who applied an explicit scheme to route floods in the Ohio River, the junction of the Ohio-Mississippi Rivers, and the Kentucky Reservoir. Among those who have studied explicit methods are Amein and Fang [1969], Martin and DeFazio [1969], Ragan [1966], Liggett and Woolhiser [1967], and Strelkoff [1970]. Also, Dronkers [1969], Balloffet [1969], Kamphuis [1970], and Prandle and Crookshank [1974] applied the explicit method to analyze tidal movement in estuaries. Garrison *et al.* [1969] and Johnson [1974] applied the explicit method to simulate flood routing in rivers and reservoirs.

Many variations of the explicit method have been developed. Some were developed specifically for rapidly varying unsteady flow in which bore formation was likely, e.g., the Lax-Wendroff two-step scheme reported by Richtmyer [1957]. Other popular schemes include the leap-frog scheme, the staggered scheme, which was used by Isaacson *et al.* [1958], and the diffusion scheme, which was developed for gradually varying flows but also was adapted for discontinuous unsteady flows such as tidal bores by Terzidis [1968].

In order to illustrate the principle of the explicit method, the versatile and yet simple diffusion method is chosen. Letting K represent any variable or function, and referring to Fig. 3.7, time and spatial derivatives at node i are approximated by the following difference quotients:

$$\frac{\partial K}{\partial t} \approx \frac{K_i^{j+1} - K_i^j}{\Delta t} \quad (3.48)$$

$$\frac{\partial K}{\partial x} \approx \frac{K_{i+1}^j - K_{i-1}^j}{2\Delta x} \quad (3.49)$$

where:

$$\bar{K}_i^j = \frac{K_{i+1}^j + K_{i-1}^j}{2} \quad (3.50)$$

All non-derivative terms are approximated by Equation (3.50). Equation (3.48) is a forward difference approximation for the time derivative, and Equation (3.49) is a central difference approximation for the spatial derivative. Two properties of the diffusion scheme should be noted. First, the scheme is explicit since the spatial derivatives and non-derivative approximations are evaluated at the time line t^j and are therefore known. The only unknown is the K_i^{j+1} term in the time derivative. The second distinguishing property is the use of the average value of K_i^j (Equation (3.50)) in the time derivative. This expression characterizes the diffusion property of this particular explicit difference scheme. Should K_i^j be replaced by K_i^j , the scheme would be numerically unstable, which illustrates the subtleties of finite difference solutions.

The conservation form of the Saint-Venant equations is chosen for applying the diffusion explicit solution scheme, these equations which were previously presented as Equations (2.55) and (2.56) are presented here for convenience, with A_0 neglected, β taken as unity, and the eddy loss S_e and wind effect W_f neglected, i.e.,

$$\frac{\partial Q}{\partial x} + \frac{\partial A}{\partial t} - q = 0 \quad (3.51)$$

$$\frac{\partial Q}{\partial t} + \frac{\partial Q^2/A}{\partial x} + gA \left(\frac{\partial h}{\partial x} + S_f \right) - q v_x = 0 \quad (3.52)$$

Before they can be approximated by explicit diffusion difference approximations, the term $\partial A/\partial t$ in Equation (3.51) must be replaced by:

$$\frac{\partial A}{\partial t} \approx B \frac{\partial y}{\partial t} \quad (3.53)$$

where y is the depth of flow and is related to the water surface elevation h by the expression:

$$y = h - z \quad (3.54)$$

in which z is the elevation of the channel bottom above a known datum. Also, it is necessary to replace the term $\partial h/\partial x$ in Equation (3.52) by the expression:

$$\frac{\partial h}{\partial x} = \frac{\partial y}{\partial x} - s_o \quad (3.55)$$

Substituting Equation (3.53) in Equation (3.51) and dividing through by B yields:

$$\frac{\partial y}{\partial t} + \frac{1}{B} \frac{\partial Q}{\partial x} - \frac{q}{B} = 0 \quad (3.56)$$

Substituting Equation (3.55) in Equation (3.52) yields:

$$\frac{\partial Q}{\partial t} + \frac{\partial Q^2/A}{\partial x} + gA \left(\frac{\partial y}{\partial x} - S_o + S_f \right) - qv_x = 0 \quad (3.57)$$

Upon substituting the diffusion difference expressions given by Equations (3.48)-(3.50) in Equations (3.56) and (3.57), the following algebraic difference equations are obtained:

$$\frac{y_i^{j+1} - \frac{1}{2} (y_{i+1}^j + y_{i-1}^j)}{\Delta t} + \frac{1}{\frac{1}{2} (B_{i+1}^j + B_{i-1}^j)} \left[\left[\frac{Q_{i+1}^j - Q_{i-1}^j}{2\Delta x} \right] - \frac{1}{2} (q_{i+1/2}^j + q_{i-1/2}^j) \right] = 0 \quad (3.58)$$

$$\frac{Q_i^{j+1} - \frac{1}{2} (Q_{i+1}^j + Q_{i-1}^j)}{\Delta t} + \frac{(Q^2/A)_{i+1}^j - (Q^2/A)_{i-1}^j}{2\Delta x} + g \frac{1}{2} (A_{i+1}^j + A_{i-1}^j) \left[\frac{y_{i+1}^j - y_{i-1}^j}{2\Delta x} - S_o + \frac{1}{2} (S_{f_{i+1}}^j + S_{f_{i-1}}^j) \right] - \frac{1}{2} (qv_x)_{i+1/2}^j + (qv_x)_{i-1/2}^j = 0 \quad (3.59)$$

All terms having a j superscript are known either from the initial condition of flow just prior to the application of the Saint-Venant unsteady flow equations or from a previous unsteady flow solution. The only unknowns are those terms having a j+1 superscript, namely y_i^{j+1} in Equation (3.58) and Q_i^{j+1} in Equation (3.59). Solving Equation (3.58) for y_i^{j+1} , we obtain:

$$y_i^{j+1} = \frac{1}{2} (y_{i+1}^j + y_{i-1}^j) - \frac{\Delta t}{\frac{1}{2} (B_{i+1}^j + B_{i-1}^j)} \left[\frac{Q_{i+1}^j - Q_{i-1}^j}{2\Delta x} - \frac{1}{2} (q_{i+1/2}^j + q_{i-1/2}^j) \right] \quad (3.60)$$

Solving Equation (3.59) for Q_i^{j+1} , we obtain:

$$\begin{aligned}
 Q_i^{j+1} = & \frac{1}{2}(Q_{i+1}^j + Q_{i-1}^j) - \frac{\Delta t}{2\Delta x} \left[(Q^2/A)_{i+1}^j - (Q^2/A)_{i-1}^j \right] \\
 & - \frac{g\Delta t}{2}(A_{i+1}^j + A_{i-1}^j) \left[\frac{y_{i+1}^j - y_{i-1}^j}{2\Delta x} - S_o + \frac{1}{2}(S_{f_{i+1}}^j + S_{f_{i-1}}^j) \right] \\
 & + \frac{\Delta t}{2} \left[(qv_x)_{i+1/2}^j + (qv_x)_{i-1/2}^j \right] = 0 \quad (3.61)
 \end{aligned}$$

Thus, Equations (3.60) and (3.61) provide a direct solution for y_i^{j+1} and Q_i^{j+1} , which can be used to obtain all the values for y and Q on the time line $j+1$. These values are then denoted by the j superscript and the next time line (denoted as $j+2$ in Fig. 3.7) is considered as the unknown time line $j+1$ in the application of Equations (3.60) and (3.61). In this way, the depth y and discharge Q are determined for all nodes along the channel and forward into the time domain.

The numerical stability of the simple diffusion difference scheme has been analyzed by a number of investigators. Terzidis [1968] applied the so-called von Neumann method of analyzing a linearized version of Equations (3.51) and (3.52) and found that the time step Δt must be restricted in size to provide numerical stability. The restriction in Δt is given by the lesser of the following two inequalities:

$$\Delta t \leq \frac{\Delta x_i}{\left(\frac{Q}{A}\right)_i + \sqrt{g\left(\frac{A}{B}\right)_i}} \quad \text{[minimum for all } i \text{]} \quad (3.62)$$

$$\Delta t \leq \frac{2.208 A_i R_i^4}{g n_i^2 |Q_i|} \quad \text{[minimum for all } i \text{]} \quad (3.63)$$

where R is the hydraulic radius.

The inequality given by Equation (3.62) is known as the Courant condition after the pioneering work of Courant et al. [1948]. It is derived for a frictionless flow and is dependent upon the flow velocity and the celerity (propagation speed) of small disturbances. When friction is considered, the second inequality given by Equation (3.63) is derived in addition to the Courant condition. Equations (3.62) and (3.63) or some slight modification are applicable to most explicit schemes.

Inspection of the stability criteria of Equation (3.62) indicates that the computational time step is substantially reduced as the hydraulic depth (A/B) increases. Thus, in deep rivers, it is not uncommon for time steps on the order of a few minutes or even seconds to be required for numerical stability even though the flood wave may be very gradual having a duration in the order of weeks. Such small time steps cause the explicit method to be very inefficient in the use of computer time.

Another restriction of explicit schemes is the use of equal Δx distance steps. Although this can be relaxed somewhat by using weighting factors, it can be disadvantageous for flows in natural river systems.

Implicit Finite Difference Methods

The term implicit refers to those finite difference schemes that advance the solution of the Saint-Venant equations from one time line to the next simultaneously for all points along the time line (i.e., along the x -axis of the channel). Thus, in an implicit method, a system of $2N$ algebraic equations is generated from the Saint-Venant equations applied simultaneously to the N net points along the x -axis. The system of algebraic equations so generated may be either linear or non-linear depending upon the type of implicit method chosen. This aspect will be discussed later.

Implicit methods of finite differences were developed because of the limitations on the size of the time step required for numerical stability of explicit methods. The use of implicit schemes to obtain solutions of the Saint-Venant equations was suggested by Isaacson et al. [1956] and first appeared in the literature in the early 1960's with the work of Preissmann [1961], Preissmann and Cunge [1961], and Vasiliev et al. [1965]. Later, Isaacson [1966], Abbott and Ionescu [1967], Amein [1968], Baltzer and Lai [1968], Dronkers [1969], Amein and Fang [1970], Gunaratnam and Perkins [1970], Kamphuis [1970], Contractor and Wiggert [1972], Quinn and Wylie [1972], Fread [1973b,c], Chen [1973], Chaudhry and Contractor [1973], Fread [1974a,b], Greco and Panattoni [1975], Amein [1975], Amein and Chu [1975], Chen and Simons [1975], and Fread [1976] reported their research with implicit methods for solving the Saint-Venant equations.

An essential difference between explicit and implicit methods is the implicit methods are computationally stable for all Δt time steps while explicit methods are numerically stable for those time steps less than the critical value determined by the Courant condition, Equation (3.62), or the friction criteria, Equation (3.63). Analyses of the numerical stability of various implicit finite difference schemes applied to the Saint-Venant equations have been reported by Abbott and Ionescu [1967], Leendertse [1967], Dronkers [1969], Gunaratnam and Perkins [1970], Fread [1974a], and Liggett and Cunge [1975]. Within the simplifications required in making the numerical stability analyses, the various implicit methods were found to be unconditionally

linearly stable, i.e., the simplified linearized versions of the Saint-Venant equations were numerically stable independent of the size of the time or distance steps. Amein and Fang [1970] and Fread [1973b] reported that extensive numerical experiments indicated the implicit method applied to the complete Saint-Venant equations was numerically stable for a wide range of time and distance steps; however, Fread [1973b] and Chaudhry and Contractor [1973] found that instability could be encountered for certain types of four-point schemes if the time steps were abnormally large for the case of rapidly varying transients.

Another basic difference between explicit and implicit methods is the latter is more computationally complex than the former. Depending on the type of implicit method (linear vs. non-linear), the number of computations during a time step increases by a factor of approximately 1.5 to 3.0 compared to the requirements of an explicit method. This increase is much greater if the method of solving the system of simultaneous equations is not an efficient method which makes use of the banded structure of the coefficient matrix of the system of equations. If the implicit method is linear, only one solution of the system of equations is required at each time step. However, if the implicit method is non-linear, an iterative solution is necessary, and this requires one or more solutions of the system of equations at each time step.

Although many variations of the implicit method have been developed, most of them can be categorized as four-point or six-point schemes which may be applied to the Saint-Venant equations so as to produce linear or non-linear difference equations.

The four-point scheme is shown in Fig. 3.8. The spatial derivatives and non-derivative terms are positioned between adjacent time lines at point M by weighting factors of θ and $(1-\theta)$, where θ is defined in Fig. 3.8 as $\Delta t'/\Delta t$. Letting K represent any variable, time and spatial derivatives at point M are approximated by the following difference quotients:

$$\frac{\partial K}{\partial t} \approx \frac{\frac{1}{2}(K_i^{j+1} + K_{i+1}^{j+1})}{\Delta t} - \frac{\frac{1}{2}(K_i^j + K_{i+1}^j)}{\Delta t} \quad (3.64)$$

$$\frac{\partial K}{\partial x} \approx \frac{\theta(K_{i+1}^{j+1} - K_i^{j+1})}{\Delta x} + \frac{(1-\theta)(K_{i+1}^j - K_i^j)}{\Delta x} \quad (3.65)$$

and non-derivative terms at point M are approximated by:

$$K \approx \frac{\theta(K_i^{j+1} + K_{i+1}^{j+1})}{2} + \frac{(1-\theta)(K_i^j + K_{i+1}^j)}{2} \quad (3.66)$$

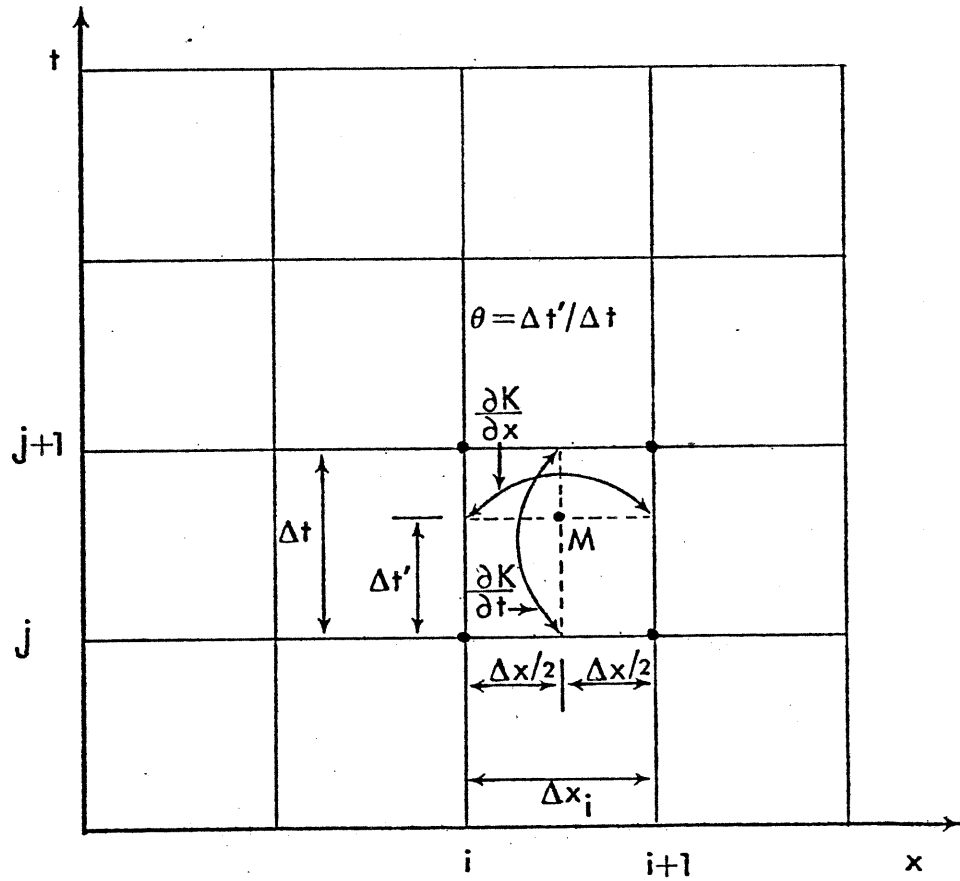


Fig. 3.8.--Weighted four-point implicit scheme.

The four-point scheme is implicit for any value of Θ greater than zero and explicit if Θ is zero. A Θ of 0.5 yields the so-called "box scheme" used by Amein and Fang [1970], Contractor and Wiggert [1972], and Fread [1973c]. A fully implicit or backward difference scheme results when Θ takes on the value of unity. The fully implicit scheme was used by Baltzer and Lai [1968], Kaumphis [1970], and Amein and Chu [1975]. The generalized weighted four-point scheme in which Θ is retained as a variable in the formulation of the difference approximation of the Saint-Venant equations was first used by Priessmann [1960] and later by Quinn and Wylie [1972], Fread [1973b, 1974a, 1974b, 1976] and Chaudhry and Contractor [1973].

The weighted four-point scheme as shown by Fread [1974a] is unconditionally linearly stable for any time step size if Θ obeys the inequality $0.5 \leq \Theta \leq 1.0$. Also, the scheme has second-order accuracy when $\Theta = 0.5$ and has only first-order accuracy when $\Theta = 1.0$.

The four-point scheme has been applied to the Saint-Venant equations such that the resulting difference equations are either non-linear or linear. The formulation of the non-linear difference equations is straight forward and results when the difference approximations, Equations (3.64)-(3.66), are substituted directly into the Saint-Venant equations. However, the linear formulation requires the linearization of non-linear terms in the Saint-Venant equations by: (1) modifying the partial differential equations so that they do not contain non-linear terms and (2) using finite difference expressions which linearize the non-linear terms. The non-linear formulation using the four-point scheme was investigated by Baltzer and Lai [1968], Amein and Fang [1970], Contractor and Wiggert [1972], Quinn and Wylie [1972], Fread [1973b, 1974a], and Amein and Chu [1975] among others. The linear formulation was used by Preissmann [1961], Preissmann and Cunge [1961], Strelkoff [1970], Chen [1973], and Chen and Simons [1975].

The weighted six-point scheme is shown in Fig. 3.9. Again, using K to represent any variable, the time and spatial derivatives are approximated at point M by the following difference quotients:

$$\frac{\partial K}{\partial t} \approx \frac{K_i^{j+1} - K_i^j}{\Delta t} \quad (3.67)$$

or

$$\frac{\partial K}{\partial t} \approx \frac{1}{2} \left[\frac{(K_{i+1}^{j+1} - K_{i+1}^j)}{\Delta t} + \frac{(K_{i-1}^{j+1} - K_{i-1}^j)}{\Delta t} \right] \quad (3.68)$$

$$\frac{\partial K}{\partial x} \approx \frac{\Theta(K_{i+1}^{j+1} - K_{i-1}^{j+1})}{2\Delta x} + \frac{(1-\Theta)(K_{i+1}^j - K_{i-1}^j)}{2\Delta x} \quad (3.69)$$

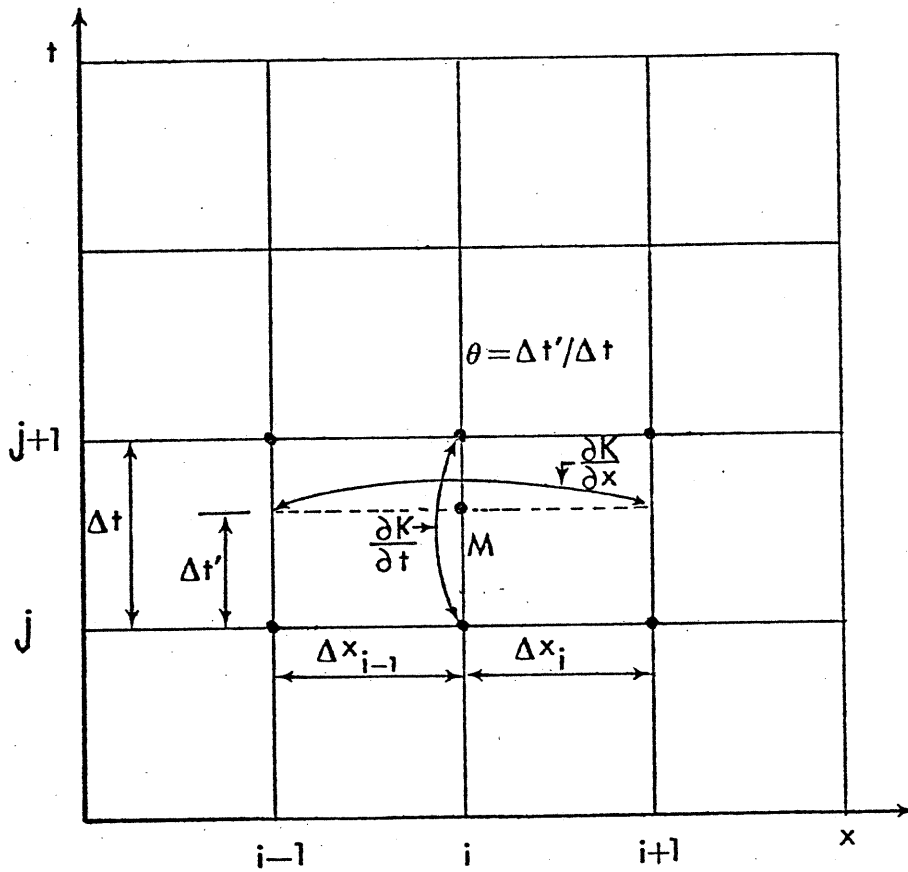


Fig. 3.9.—Weighted six-point implicit scheme.

and non-derivative terms at point M are approximated by:

$$K = \theta K_i^{j+1} + (1-\theta) K_i^j \quad (3.70)$$

The six-point scheme is implicit for any value of θ greater than zero. It is unconditionally linearly stable if θ obeys the inequality $0.5 \leq \theta \leq 1.0$. The convergence properties of the six-point scheme are similar to those of the four-point scheme. A non-linear six-point scheme with $\theta = 0.5$ was investigated by Abbott and Ionescu [1966] and a linearized six-point scheme with $\theta = 1.0$ was proposed by Vasiliev et al. [1965]. Both of the six-point schemes used by Abbott and by Vasiliev treat the boundary conditions in a more complicated and less desirable manner than they are treated in the four-point schemes. Also, the six-point schemes are not as well suited to irregular Δx distance intervals as the four-point schemes.

Application of an implicit scheme to the Saint-Venant will not be illustrated in this section since such an application is presented in detail in the preceding section.

4. WEIGHTED FOUR-POINT IMPLICIT METHOD

Introduction

In this section, the weighted four-point scheme is used to obtain an implicit finite difference solution of the conservation form of the Saint-Venant Equations (2.55) and (2.56), which are repeated here for convenient reference, i.e.,

$$\frac{\partial Q}{\partial x} + \frac{\partial(A + A_o)}{\partial t} - q = 0 \quad (4.1)$$

$$\frac{\partial Q}{\partial t} + \frac{\partial(\beta Q^2/A)}{\partial x} + gA\left(\frac{\partial h}{\partial x} + S_f + S_e\right) - \beta q v_x + W_f B = 0 \quad (4.2)$$

The conservation form of the Saint-Venant equations is chosen because this form provides the versatility required to simulate a wide range of flows from gradual long-duration flood waves in rivers to abrupt waves such as caused by dam breaks. The conservation form of the differential type Saint-Venant equations when approximated by finite differences results in equations resembling the "integral" version of the unsteady flow equations [Liggett, 1975] rather than the differential form as developed in section 2. In the integral form of the unsteady flow equations, the dependent variables Q and h do not have to be continuous as is necessary in the differential form of the Saint-Venant Equations (4.1) and (4.2). Since the finite difference form of Equations (4.1) and (4.2) mimics the integral form of the unsteady flow equations, the water surface h may be discontinuous, in a finite sense, as in the case of waves having abrupt faces.

The weighted four-point implicit scheme is chosen rather than an explicit scheme. Explicit methods, although simpler in application than implicit methods, are not suitable for simulation of long-term unsteady flow phenomena such as flood waves in rivers because they are restricted by mathematical stability considerations to very small Δt computational time steps (on the order of a few minutes) as governed by Equations (3.62) and (3.63). Such small time steps cause the explicit methods to be very inefficient in the use of computer time. Implicit finite difference techniques, however, have no restrictions on the size of the time step due to mathematical stability; however, convergence considerations may require time steps to be limited to something less than a few hundred times that required by an explicit method, depending on the hydraulic properties of the unsteady flow phenomena and the size of the Δx distance step.

The implicit method is preferred over the method of characteristics because the former enables a more direct approach for simulating unsteady flows in natural channels such as rivers, reservoirs, and estuaries. Such natural channels have irregular cross-sections, off-channel storages, and the practical requirement for unequal

distance steps. Each of these introduces unwarranted complications into the method of characteristics which detract from any of its inherent advantages pertaining to stability and convergence.

Of the various implicit schemes that have been developed, the weighted four-point scheme first used by Preissmann [1961] and recently by Quinn and Wylie [1973], Chaudry and Contractor [1973], and Fread [1973c, 1974b, 1976] is considered most advantageous since it can readily be used with unequal distance steps and its stability-convergence properties can easily be controlled.

The weighted four-point difference approximations are applied directly to Equations (4.1) and (4.2) which results in a system of algebraic non-linear difference equations. Although linear four-point implicit formulations such as advocated by Chen and Simons [1975] and others do not necessitate an iterative solution of the system of equations, the option of a non-iterative solution procedure is available with the four-point non-linear formulation. This arises from the way in which the Newton-Raphson procedure for solving systems of non-linear equations is applied. The manner in which the non-linear formulation mimics the linear formulation will become apparent when the Newton-Raphson solution procedure is described later in this section. Thus, the non-linear formulation possesses its own inherent advantages while still allowing the computational advantage associated with the linear formulation.

Numerical Properties

The numerical properties (stability and convergence) of the weighted four-point implicit scheme have been investigated by Cunge [1966], Fread [1973b, 1974a], and Chaudry and Contractor [1973].

Some investigations [Fread, 1973b; Chaudry and Contractor, 1973] were based on numerical experiments to determine the four-point scheme's numerical properties in an empirical manner. Although numerical experiments enable the investigator to study the four-point scheme applied to the complete Saint-Venant equations, the findings are limited to the range of conditions studied.

Other investigators [Cunge, 1966; Fread, 1974a] used analytical techniques to investigate the four-point scheme's numerical properties. Although the results from analytical techniques are applicable over a broad range of conditions, the complete Saint-Venant equations must be linearized and somewhat simplified before the four-point scheme is applied. Thus, the results of the analytical investigation are, in the strictest sense, only applicable to the linearized equations; however, experience has proven that considerable understanding of the numerical properties of non-linear equations can be attained from this kind of analysis.

The following is a summary of the numerical properties of the weighted four-point scheme as reported by Fread [1974a]. The four-point scheme as described by Equations (3.64)-(3.66) was applied to the following linearized model of the complete non-linear Saint-Venant equations:

$$\frac{\partial h}{\partial t} + H_0 \frac{\partial v}{\partial x} = 0 \quad (4.3)$$

$$\frac{\partial v}{\partial t} + g \frac{\partial h}{\partial x} + kv = 0 \quad (4.4)$$

in which k is the linearized friction term given by:

$$k = \frac{g \cdot V_0 n^2}{1.1 H_0^{4/3}} \quad (4.5)$$

where v is a small perturbation in velocity above a mean velocity V_0 , h is a small perturbation in depth above a mean depth H_0 , g is the acceleration due to gravity, and n is Manning's roughness coefficient.

The stability of the four-point scheme applied to Equations (4.3) and (4.4) was analyzed using the von Neumann technique [O'Brien *et al.*, 1951]. An expression for stability (in the sense of the von Neumann conjecture that linear operators with variable coefficients are stable if all their localized operators in which the coefficients are taken constant are stable) is given by the following expression:

$$|\lambda| = \left(\frac{1 + (2\theta - 2)^2 a + (\theta - 1)b}{1 + 4\theta^2 a + \theta b} \right)^{1/2} \quad (4.6)$$

in which:

$$a = g H_0 (\Delta t / \Delta x)^2 \tan^2 (\pi \Delta x / L) \quad (4.7)$$

$$b = k \Delta t \quad (4.8)$$

where L is the wave length, i.e., the wave celerity times the duration of the wave. If $|\lambda| < 1$, independent of the values of Δx and Δt , the errors due to truncation and round-off will not grow with time and the difference equations are unconditionally linearly stable. This is the case when $1/2 < \theta \leq 1$. The scheme is weakly stable (i.e., $|\lambda| = 1$) when $\theta = 1/2$ and k approaches zero. Thus, when friction is negligible, the solution tends to oscillate about the true solution; and since the oscillations are bounded and are not large relative to the solution, the condition is not an unstable one but rather is known as a "computational mode." If θ is increased to about 0.55 or 0.60, the computational mode is eliminated.

The convergence properties of the weighted four-point scheme were investigated qualitatively in terms of a truncation error, E, which was found to have the following form:

$$E = (2\theta-1) O(\Delta t) + O(\Delta t)^2 + O(\Delta x)^2 \quad (4.9)$$

where O indicates "order of." When θ is unity, the truncation error is:

$$E = O(\Delta t) + O(\Delta t)^2 + O(\Delta x)^2 \quad (4.10)$$

which clearly shows that the fully implicit scheme has only first-order accuracy due to the presence of the term $O(\Delta t)$. When θ is 1/2 the truncation error is:

$$E = O(\Delta t)^2 + O(\Delta x)^2 \quad (4.11)$$

which shows the box scheme to have higher (second-order) accuracy. As θ departs from 1/2 and approaches unity, the scheme changes from second order to first order as the leading coefficient $(2\theta-1)$ of the first-order term increases from zero to unity.

Convergence of the weighted four-point scheme was further investigated quantitatively using a Fourier technique similar to that used by Leendertse [1967] in which convergence ratios of the finite difference solution to the analytical solution were determined for wave damping (attenuation) and celerity (velocity). The following expression of the damping C_d and celerity C_c convergence ratios were obtained:

$$C_d = \frac{\left[\frac{1 + (2\theta-2)^2 (D_c \tan \pi/D_L)^2 + (\theta-1) D_f}{1 + 4\theta^2 (D_c \tan \pi/D_L)^2 + \theta D_f} \right]^{1/2}}{e^{(-0.5 D_f)}} \quad (4.12)$$

$$C_c = \frac{\tan^{-1} \left[\frac{\sqrt{16 (D_c \tan \pi/D_L)^2 - D_f^2}}{2 + 8\theta (\theta-1) (D_c \tan \pi/D_L)^2 + (2\theta-1) D_f} \right]}{\frac{2\pi}{D_L} D_c \sqrt{1 - (0.5 D_f)^2}} \quad (4.13)$$

in which:

$$D_L = L/\Delta x \quad (4.14)$$

$$D_c = \frac{\Delta t}{\Delta x} \sqrt{g H_o} \quad (4.15)$$

$$D_f = k\Delta t \quad (4.16)$$

and the parameters L , H_0 , and k are as previously defined in connection with Equations (4.3)-(4.5).

In Fig. 4.1, the convergence ratios C_d and C_c are shown plotted for a range of values of D_c (the Courant number) and D_L (the wave discretization number) with $\Theta = 0.5$ and $D_f = 0.0$. The damping convergence ratio C_d is unity for all D_c and D_L values, i.e., there is no numerical damping for any choice of Δx and Δt when $\Theta = 0.5$ and friction is negligible. However, the celerity convergence ratio C_c approaches unity only when D_L becomes large for all D_c values greater than unity, i.e., the numerical celerity approaches the analytical celerity for time steps greater than that defined by the Courant condition ($D_c = 1$) as the wave discretization number becomes large (small values of Δx relative to the wave length L).

The importance of the Θ parameter is illustrated by the convergence ratios shown in Fig. 4.2. A comparison of the C_d curves in Fig. 4.2 where $\Theta = 1.0$ and $D_f = 0.0$ with those in Fig. 4.1 where $\Theta = 0.5$ and $D_f = 0.0$ clearly shows the increase in numerical damping errors due to the Θ parameter increasing from 0.5 to 1.0. A comparison of the C_c curves in Figs. 4.1 and 4.2 also shows some increase in the numerical celerity errors when the Θ parameter is increased from 0.5 to 1.0.

Fig. 4.3 shows the convergence ratios with $\Theta = 0.5$ and $D_f = 1.0$. It is apparent that C_d only approaches unity as D_L increases. As D_c increases, larger values of D_L are required for C_d to approach unity. The celerity convergence ratio C_c , in Fig. 4.3, is slightly different from the C_c curves of Fig. 4.1. The increase in the dimensionless friction parameter D_f causes the C_c curves in Fig. 4.3 to be slightly displaced to the left of those in Fig. 4.1, which indicates that as friction increases numerical errors in the celerity are reduced for given values of Δx and Δt .

A summary view of the numerical properties of the weighted four-point implicit scheme indicates that:

1. The scheme is unconditionally stable for $0.5 \leq \Theta \leq 1.0$.
2. The scheme is most accurate when $\Theta = 0.5$ and least accurate when $\Theta = 1.0$.
3. The weakly stable condition associated with $\Theta = 0.5$ when friction is negligible can be avoided by increasing Θ to about 0.55 and thereby minimizing the loss of accuracy as Θ departs from 0.5.

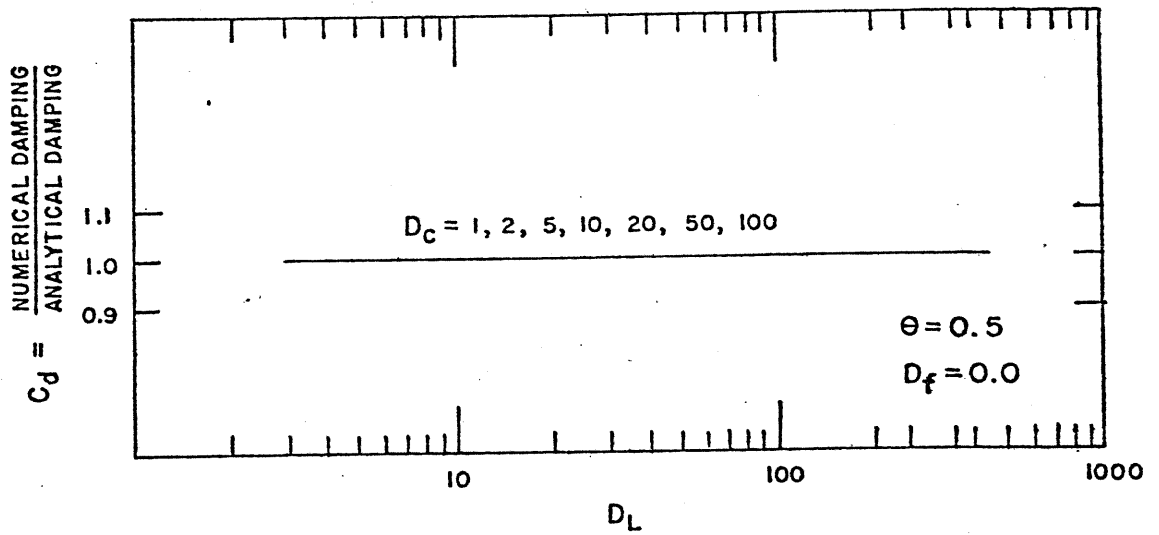


Fig. 4.1.a.--Damping convergence ratio, C_d , against D_L for box scheme with variations in D_c and $D_f = 0.0$.

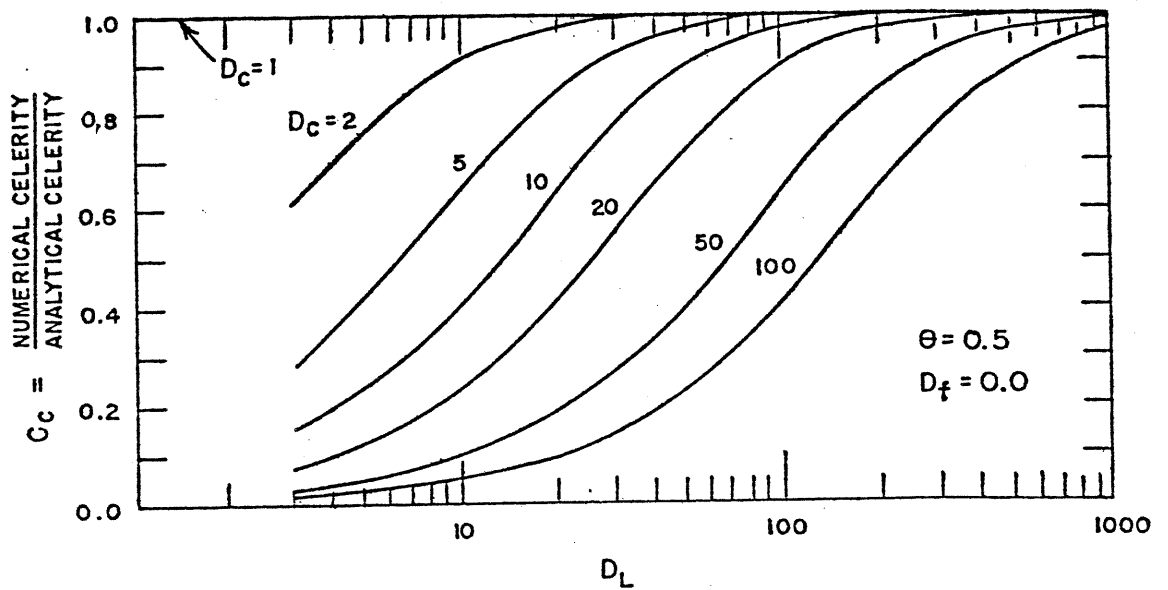


Fig. 4.1.b.--Celerity convergence ratio, C_c , against D_L for box scheme with variations in D_c and $D_f = 0.0$.

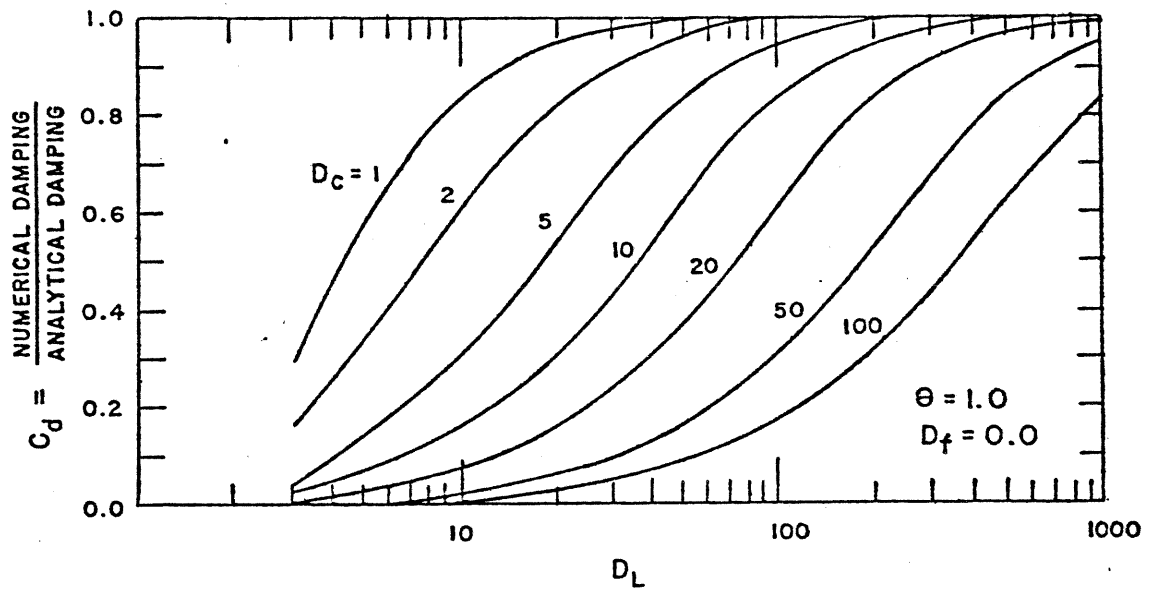


Fig. 4.2.a.--Damping convergence ratio, C_d , against D_L for backward implicit scheme with variations in D_c and $D_f = 0.0$.

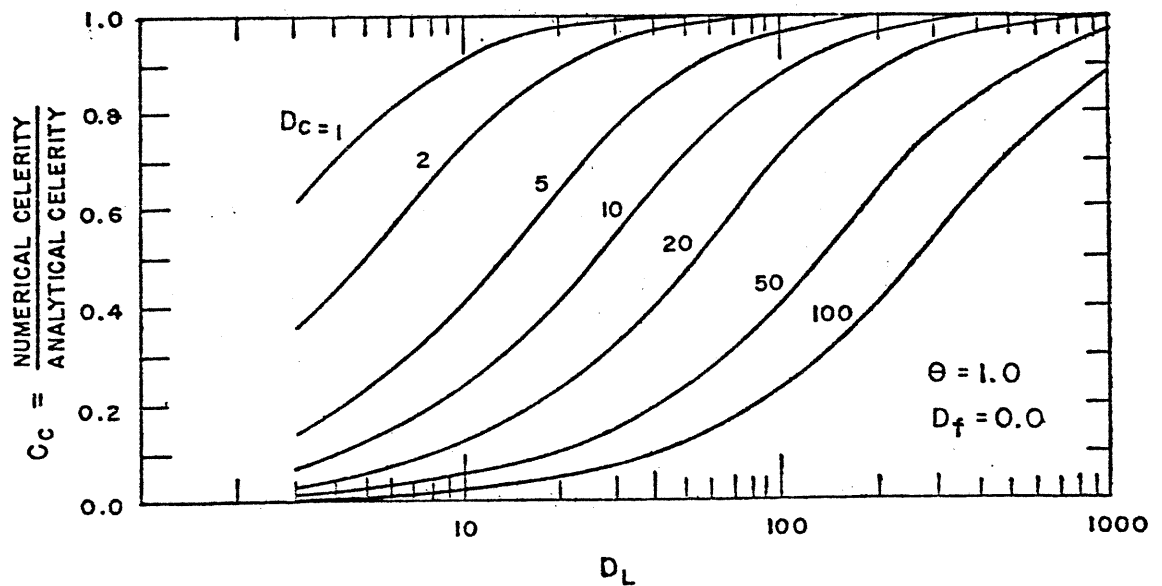


Fig. 4.2.b.--Celerity convergence ratio, C_c , against D_L for backward implicit scheme with variations in D_c and $D_f = 0.0$.

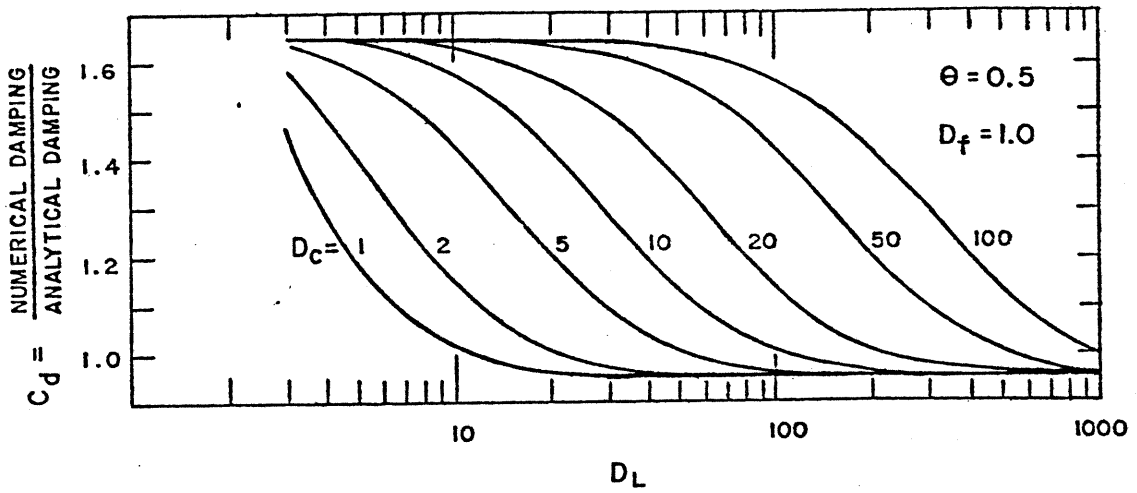


Fig. 4.3.a.--Damping convergence ratio, C_d , against D_L for box scheme with variations in D_c and $D_f = 1.0$.

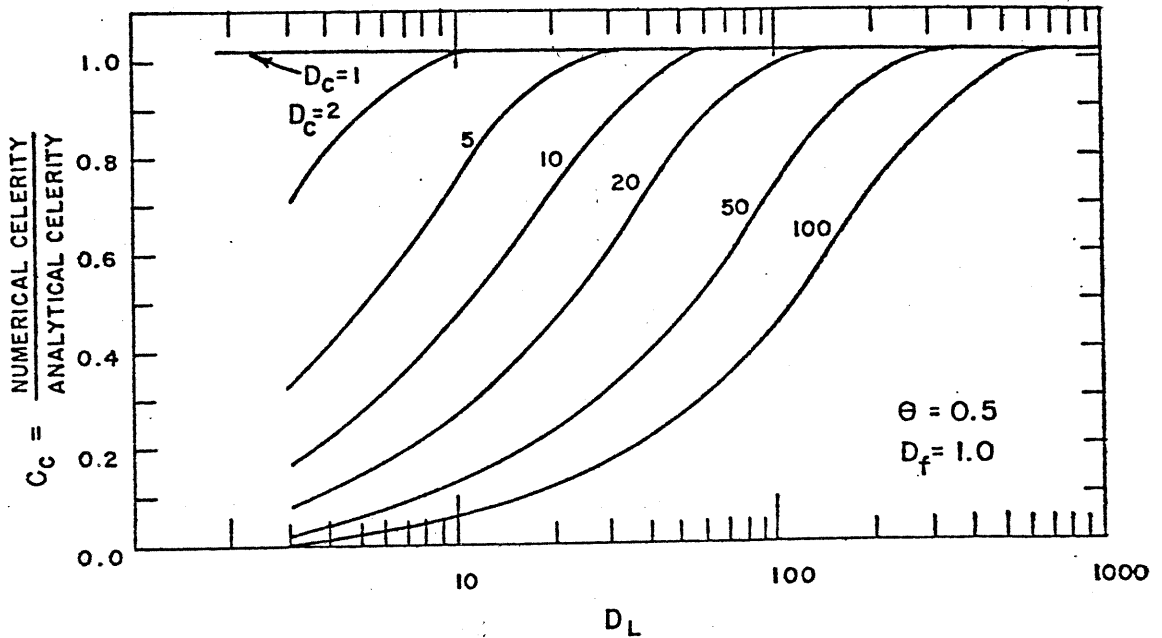


Fig. 4.3.b.--Celerity convergence ratio, C_c , against D_L for box scheme with variations in D_c and $D_f = 1.0$.

Finite Difference Equations

The weighted four-point implicit scheme is shown in Fig. 3.8. It should be recognized that the Δx distance intervals may be unequal and the Δt time intervals may also be unequal. The weighting parameter θ is defined in Fig. 3.8 as $\Delta t' / \Delta t$. The weighted four-point finite difference approximations were given by Equations (3.64)-(3.66) and are repeated here for convenient reference. Letting K represent any variable, the time derivative is approximated by:

$$\frac{\partial K}{\partial t} \approx \frac{K_i^{j+1} + K_{i+1}^{j+1} - K_i^j - K_{i+1}^j}{2\Delta t} \quad (4.17)$$

and the spatial derivatives and non-derivative terms are positioned between adjacent time lines according to weighting factors of θ and $(1-\theta)$ by the following approximations:

$$\frac{\partial K}{\partial x} \approx \frac{\theta(K_{i+1}^{j+1} - K_i^{j+1})}{\Delta x} + (1-\theta) \frac{(K_{i+1}^j - K_i^j)}{\Delta x} \quad (4.18)$$

$$K \approx \frac{\theta(K_i^{j+1} + K_{i+1}^{j+1})}{2} + (1-\theta) \frac{(K_i^j + K_{i+1}^j)}{2} \quad (4.19)$$

Upon substituting Equations (4.17)-(4.19) into the conservation form of the Saint-Venant Equations (4.1) and (4.2), the following difference equations are obtained:

$$\begin{aligned} & \theta \left[\frac{(Q_{i+1}^{j+1} - Q_i^{j+1})}{\Delta x_i} - q_i^{j+1} \right] + (1-\theta) \left[\frac{(Q_{i+1}^j - Q_i^j)}{\Delta x_i} - q_i^j \right] \\ & + \left[\frac{(A+A_o)_i^{j+1} + (A+A_o)_{i+1}^{j+1} - (A+A_o)_i^j - (A+A_o)_{i+1}^j}{2\Delta t_j} \right] = 0 \end{aligned} \quad (4.20)$$

$$\begin{aligned}
& \frac{(Q_i^{j+1} + Q_{i+1}^{j+1} - Q_i^j - Q_{i+1}^j)}{2\Delta t_j} + \Theta \left\{ \frac{(\beta Q^2/A)_{i+1}^{j+1} - (\beta Q^2/A)_i^{j+1}}{\Delta x_i} \right. \\
& + g_{A_i}^{j+1} \left[\frac{(h_{i+1}^{j+1} - h_i^{j+1})}{\Delta x_i} + \bar{S}_{f_i}^{j+1} + \bar{S}_{e_i}^{j+1} \right] - (\overline{\beta q v_x})_i^{j+1} + (\overline{W_f B})_i^{j+1} \left. \right\} \\
& + (1-\Theta) \left\{ \frac{(\beta Q^2/A)_{i+1}^j - (\beta Q^2/A)_i^j}{\Delta x_i} + g_{A_i}^j \left[\frac{(h_{i+1}^j - h_i^j)}{\Delta x_i} + \bar{S}_{f_i}^j + \bar{S}_{e_i}^j \right] \right. \\
& \left. - (\overline{\beta q v_x})_i^j + (\overline{W_f B})_i^j \right\} = 0 \tag{4.21}
\end{aligned}$$

Upon multiplying Equation (4.20) and (4.21) by Δx_i , the following are obtained:

$$\begin{aligned}
& \Theta \left(Q_{i+1}^{j+1} - Q_i^{j+1} - \bar{q}_i^{j+1} \Delta x_i \right) + (1-\Theta) \left(Q_{i+1}^j - Q_i^j - \bar{q}_i^j \Delta x_i \right) \\
& + \left(\frac{\Delta x_i}{2\Delta t_j} \right) \left[(A+A_o)_{i+1}^{j+1} + (A+A_o)_i^{j+1} - (A+A_o)_i^j - (A+A_o)_{i+1}^j \right] = 0 \tag{4.22}
\end{aligned}$$

$$\begin{aligned}
& \left(\frac{\Delta x_i}{2\Delta t_j} \right) (Q_i^{j+1} + Q_{i+1}^{j+1} - Q_i^j - Q_{i+1}^j) + \Theta \left[(\beta Q^2/A)_{i+1}^{j+1} - (\beta Q^2/A)_i^{j+1} \right. \\
& + g_{A_i}^{j+1} \left[h_{i+1}^{j+1} - h_i^{j+1} + \bar{S}_{f_i}^{j+1} \Delta x_i + \bar{S}_{e_i}^{j+1} \Delta x_i \right] \\
& \left. - (\overline{\beta q v_x})_i^{j+1} \Delta x_i + (\overline{W_f B})_i^{j+1} \Delta x_i \right] + (1-\Theta) \left[(\beta Q^2/A)_{i+1}^j \right. \\
& \left. - (\beta Q^2/A)_i^j + g_{A_i}^j \left[h_{i+1}^j - h_i^j + \bar{S}_{f_i}^j \Delta x_i + \bar{S}_{e_i}^j \Delta x_i \right] \right. \\
& \left. - (\overline{\beta q v_x})_i^j \Delta x_i + (\overline{W_f B})_i^j \Delta x_i \right] = 0 \tag{4.23}
\end{aligned}$$

in which:

$$\bar{\beta}_i = \frac{\beta_i + \beta_{i+1}}{2} \tag{4.24}$$

$$\bar{A}_i = \frac{A_i + A_{i+1}}{2} \tag{4.25}$$

$$\bar{B}_i = \frac{B_i + B_{i+1}}{2} \quad (4.26)$$

$$\bar{S}_{f_i} = \frac{\bar{n}_i^2 |\bar{Q}_i| \bar{Q}_i}{2.208 \bar{A}_i^2 \bar{R}_i^{4/3}} \quad (4.27)$$

$$\bar{Q}_i = \frac{Q_i + Q_{i+1}}{2} \quad (4.28)$$

$$\bar{R}_i = \bar{A}_i / \bar{B}_i \quad (4.29)$$

$$\bar{S}_{e_i} = \frac{K_{e_i}}{2g\Delta x_i} \left[\left(\frac{Q}{A} \right)_{i+1}^2 - \left(\frac{Q}{A} \right)_i^2 \right] \quad (4.30)$$

$$\bar{W}_{f_i} = C_{w_i} (\cos \omega)^2 |\bar{V}_{r_i}| \bar{V}_{r_i} \quad (4.31)$$

$$\bar{V}_{r_i} = \pm \bar{V}_{w_i} + \bar{Q}_i / \bar{A}_i \quad (4.32)$$

The bar (—) above the variables represents the average of that particular variable over the reach length Δx_i between the net points i and $i+1$. The subscript i associated with q , v_x , A , B , S_f , Q , R , S_e , \bar{W}_f , \bar{V}_r and \bar{V}_w represents the number of the reach, (Δx_i) rather than the node number. Node numbers commence with 1 and terminate with N , while reach numbers commence with 1 and terminate with $(N-1)$.

Equation (4.22) is the four-point finite difference equation which approximates the Continuity Equation (4.1), and Equation (4.23) is the difference equation which approximates the equation of motion, Equation (4.2). All terms having a j superscript are known either from: (1) initial conditions, i.e., the state of the flow as described by h and Q for all nodes at time $t=0$ when the Saint-Venant equations first are applied, or (2) a previous solution of the Saint-Venant equations. Other terms must be specified independent of the solution and are therefore known; these are g , Δx_i , β_i , K_{e_i} , C_{w_i} , V_{w_i} . The terms A_i^{j+1} , A_{i+1}^{j+1} , B_i^{j+1} , B_{i+1}^{j+1} , n_i^{j+1} are unknown; however, they are known linear or non-linear functions of the basic unknowns which are Q_i^{j+1} , Q_{i+1}^{j+1} , h_i^{j+1} , h_{i+1}^{j+1} . Thus, of all the terms in Equations (4.22) and (4.23), there are only four that are unknown, namely Q_i^{j+1} , Q_{i+1}^{j+1} , h_i^{j+1} , h_{i+1}^{j+1} ; however, these are raised to powers other than unity such that Equations (4.22) and (4.23) are non-linear.

Since there are four unknowns and only two equations, a solution is not possible. However, if Equations (4.22) and (4.23) are applied to each of the (N-1) rectangular grids shown in Fig. 4.4 between the upstream boundary (i=1) and the downstream boundary (i=N), a system of (2N-2) non-linear equations with 2N unknowns is obtained. Then, prescribed boundary conditions, one at the upstream boundary and one at the downstream boundary, provide the necessary additional two equations required for the system of non-linear equations to be determinate.

Boundary and Initial Conditions

Boundary conditions must be specified in order to obtain solutions to the Saint-Venant equations. This was shown in section 2 in connection with the "method of characteristics" and the necessity of boundary conditions in the implicit method has been shown. In fact, in most unsteady flow problems, the unsteady disturbance is introduced into the flow system at the boundaries (extremities of the flow system as shown in Fig. 4.4) by the so-called boundary conditions.

The upstream boundary condition can be specified as:

1. A known stage hydrograph or water surface elevation in which h_1 is known as a function of time, expressed mathematically as:

$$h_1^{j+1} - h'(t^{j+1}) = 0 \quad (4.33)$$

in which $h'(t^{j+1})$ is the known water surface elevation at the upstream boundary at time t^{j+1} , or

2. A known discharge hydrograph in which Q_1 is known as a function of time, expressed mathematically as:

$$Q_1^{j+1} - Q'(t^{j+1}) = 0 \quad (4.34)$$

in which $Q'(t^{j+1})$ is the known discharge at the upstream boundary at time t^{j+1} .

Stage is related to the water surface elevation by the datum of the gage used to measure the stage. Thus:

$$h = s + G_Z \quad (4.35)$$

where s is the stage and G_Z is gage zero or elevation of the zero point on the gage above a datum plane such as mean sea level (m.s.l.).

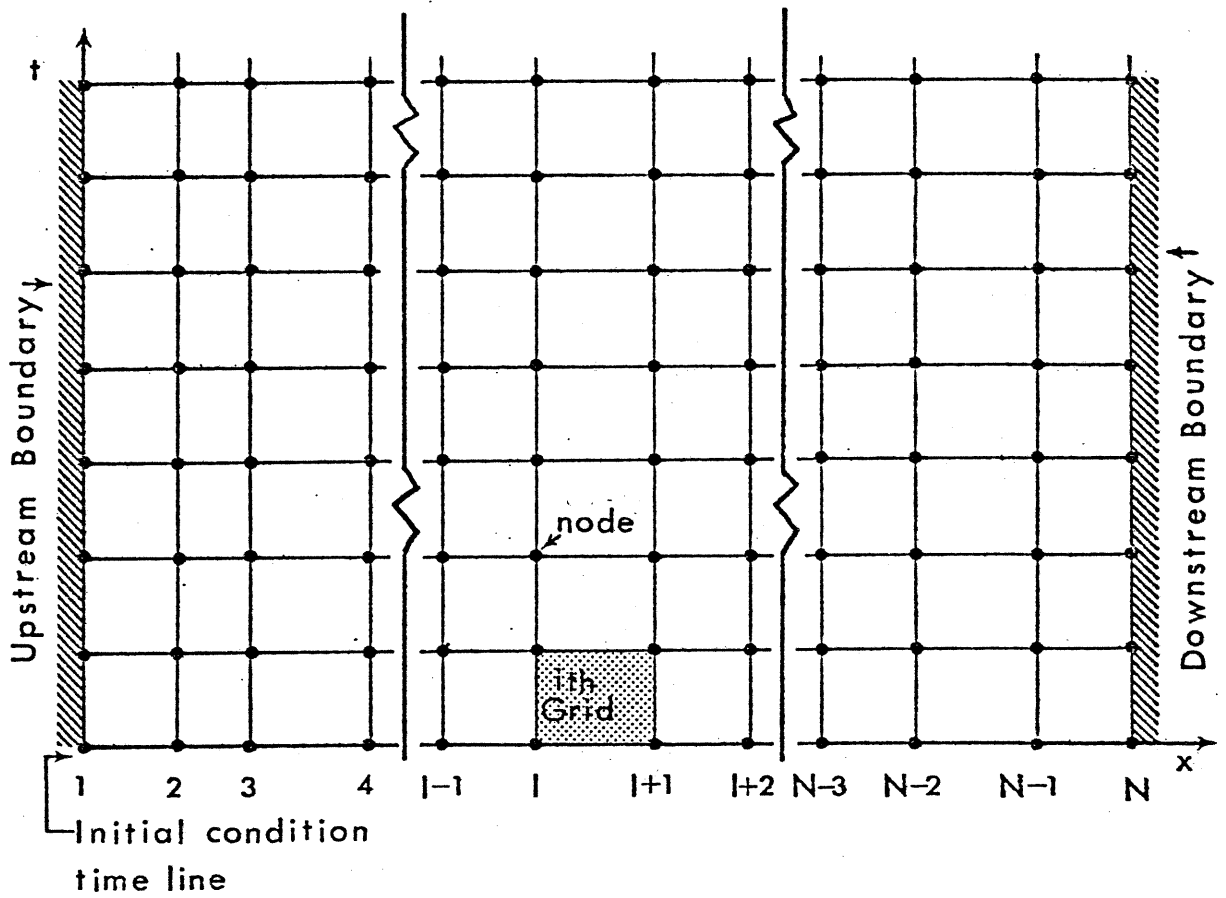


Fig. 4.4.-- $x-t$ solution plane showing time lines, nodes, grids, upstream and downstream boundaries, and initial condition time line.

Either of the upstream boundary conditions is satisfactory; the one chosen for use is determined by its availability and convenience. If $h'(t^{j+1})$ is used, $Q'(t^{j+1})$ will be determined as the Saint-Venant equations are solved at each time level, t^{j+1} . Likewise, if $Q'(t^{j+1})$ is specified, $h'(t^{j+1})$ is determined from the solution of the Saint-Venant equations at each time level, t^{j+1} .

The downstream boundary can be specified as:

1. A known stage hydrograph or water surface elevation in which h_N is known as a function of time such as an observed or predicted tide, expressed mathematically as:

$$h_N^{j+1} - h''(t^{j+1}) = 0 \quad (4.36)$$

in which $h''(t^{j+1})$ is the known water surface elevation at the downstream boundary at time t^{j+1} , or

2. A known discharge hydrograph in which Q_N is known as a function of time, expressed mathematically as:

$$Q_N - Q''(t^{j+1}) = 0 \quad (4.37)$$

in which $Q''(t^{j+1})$ is the known discharge at the downstream boundary at time t^{j+1} , or

3. A known relationship between stage and discharge such as a rating curve, expressed mathematically as:

$$Q_N^{j+1} - f(h_N^{j+1}) = 0 \quad (4.38)$$

in which $f(h_N^{j+1})$ is the rating curve or known relationship between stage and discharge.

Typical reconstitution simulations, in which stages and discharges at intermediate locations along a river are computed and compared with observations, have as an upstream boundary condition the observed stage hydrograph while the downstream boundary condition is an observed stage hydrograph also. However, the boundary conditions for a reconstitution simulation may be any combination of Equations (4.33) through (4.38). It should be recognized, however, that if discharge hydrographs are used for both the upstream and downstream boundary conditions, any error in the initial conditions (the initial water surface elevations and discharges at all computational (node) locations

along the river between the upstream and downstream boundaries when the simulation is started) will be perpetuated in the computations. This is not the case when any of the other possible combinations of boundary conditions are used. In fact, in these combinations of boundary conditions, small errors in the initial conditions will dampen as the computations proceed in time such that after a few time steps the original errors will represent a negligible portion of the computed values of h and Q .

Typical forecasting (prediction) simulations, in which the stages and discharges at points removed from the boundaries are the desired products of the computations, the upstream boundary may be either a discharge on stage hydrograph while the downstream boundary is usually a rating curve. In the case of a stage hydrograph at the upstream boundary, the initial phases of the hydrograph may be composed of observed values while the later portions of the hydrograph are the computed (predicted) values from another model applied to an upstream reach of the river above the location of the upstream boundary. Another type of forecasting simulation could have a stage hydrograph as a downstream boundary; this would occur when the downstream boundary is primarily influenced by tidal action, in which case the predicted tide would be used as the known stage hydrograph. When reservoir flows are being simulated, the upstream boundary is usually a discharge hydrograph while the downstream boundary may be a stage-discharge relation determined by natural controls or by man-operated controls according to some "rule-curve" operating procedure.

The downstream boundary condition of a stage-discharge relation may be one of several types. These include the following:

1. Single value rating curve in which the stages and corresponding discharges are expressed in tabular form with linear interpolation used for intermediate values. Such a rating curve is depicted in Fig. 4.5. The downstream boundary condition for a single value rating curve expressed in tabular (piece-wise linear) form is given by the following expression:

$$Q_N^{j+1} - \left[Q_k + \frac{(Q_{k+1} - Q_k)}{(h_{k+1} - h_k)} (h_N^{j+1} - h_k) \right] = 0 \quad (4.39)$$

where the stages and discharges in Equation (4.39) are defined in Fig. 4.5. Once the value of the expression inside the brackets of Equation (4.39) is obtained, it replaces the term $f(h_N)$ in the boundary condition given by Equation (4.38).

2. Loop rating curve in which the relation between stage and discharge is not a unique function dependent only on the values of stage and discharge but is also a function of the friction slope S_f . If S_f is approximated as the water surface slope $-(\partial h/\partial x)$, then a loop rating relationship similar to that shown in Fig. 4.6 can be computed

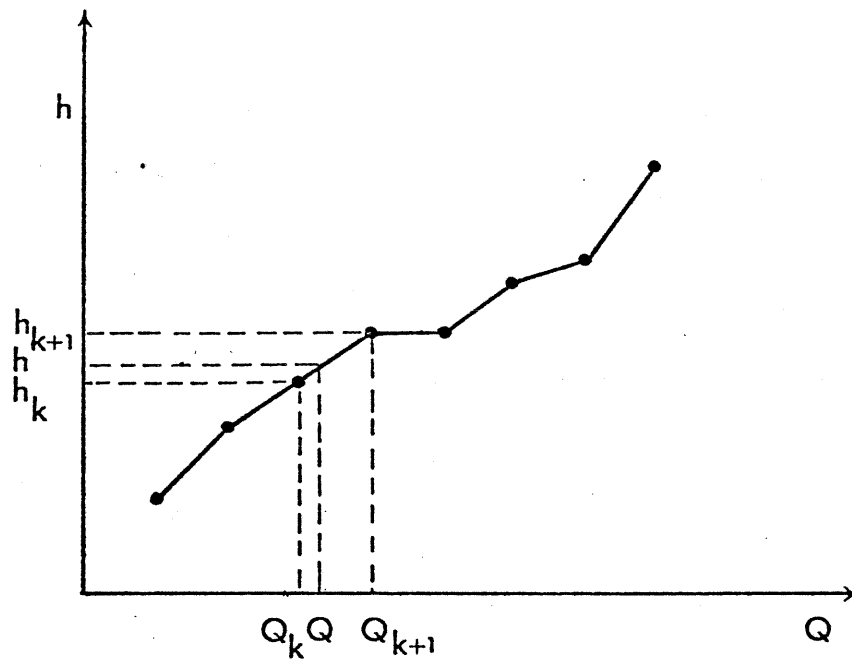


Fig. 4.5.--Single-value rating curve.

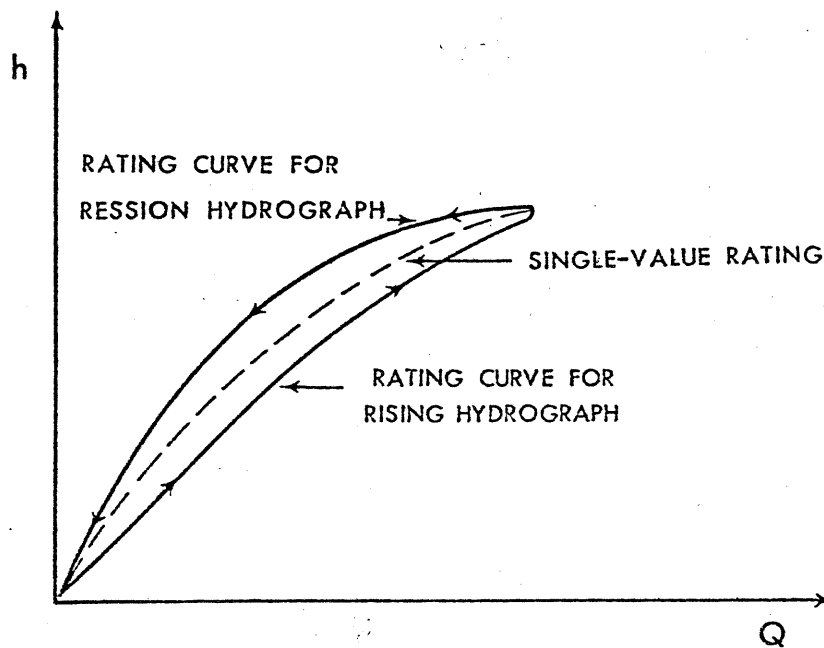


Fig. 4.6.--Loop rating curve.

[Fread, 1975b]. Since the water surface slope is greater than the channel bottom slope S_0 when the flow is increasing and less than S_0 when the flow is decreasing, the loop rating is below the single value rating on the rising limb and above it on the recession limb. Actually, if S_f is determined from the Momentum Equation (4.2), terms other than $\partial h/\partial x$ are seen to affect S_f ; however, these terms are usually small in comparison, especially for typical flood routing problems and can be safely neglected. The boundary condition for a loop rating curve is given by the following expression:

$$Q_N^{j+1} - 1.486 \left(\frac{AR^{2/3}}{n} \right)_N^{j+1} \left(\frac{h_{N-1}^{j+1} - h_N^{j+1}}{\Delta x_{N-1}} \right)^{1/2} = 0 \quad (4.40)$$

For additional information on loop rating curves, refer to [Fread, 1973c; 1975a].

3. Weir type relation between stage and discharge. This type of boundary condition can be used when the flow is controlled at the downstream boundary by some type of weir or gated structure. The boundary condition assumes the following form under this condition of flow:

$$Q_N^{j+1} - a(h_N^{j+1} - h_w)^b = 0 \quad (4.41)$$

in which a and b are coefficients depending on the type of weir and h_w is the elevation of the weir crest.

When simulating in the forecasting mode, it is important that the locations of the upstream boundary be such that the stages or discharges specified as the known boundary condition are not affected by the flow conditions downstream of this location. In either the forecasting or reconstitution mode when a rating curve is used as the downstream boundary, it is important that the location of the boundary be such that the flow at that location is not affected by flow conditions further downstream. Of course, there is always some minor influences on the flow due to the presence of cross-section irregularities downstream of a given location; however, these usually can be neglected unless the cross-section irregularity is very pronounced such as to cause significant backwater or drawdown effects. Reservoirs or major tributaries below the downstream boundary which may produce backwater effects on the rating curve at the downstream boundary location should be avoided. When this situation is unavoidable, the reach of river for which the Saint-Venant equations are being used to simulate the flow should be extended on downstream to a point below where the tributary enters or to the dam in the case of the reservoir. Of course, the routing reach can also be shortened such that the downstream boundary is shifted a sufficient distance upstream to a point where backwater effects are always negligible.

Solution of System of Difference Equations

Upon applying the difference Equations (4.22) and (4.23) to each of the (N-1) grids shown in Fig. 4.4 and including an upstream boundary equation and a downstream boundary equation, the following system of non-linear equations (expressed in functional form) is obtained:

$$\begin{aligned}
 &B_1(h_1, Q) = 0 \\
 &C_1(h_1, Q_1, h_2, Q_2) = 0 \\
 &M_1(h_1, Q_1, h_2, Q_2) = 0 \\
 &:\text{::::::::::::::::::::::::::::::::::} \\
 &C_i(h_i, Q_i, h_{i+1}, Q_{i+1}) = 0 \\
 &M_i(h_i, Q_i, h_{i+1}, Q_{i+1}) = 0 \\
 &:\text{::::::::::::::::::::::::::::::::::} \\
 &C_{N-1}(h_{N-1}, Q_{N-1}, h_N, Q_N) = 0 \\
 &M_{N-1}(h_{N-1}, Q_{N-1}, h_N, Q_N) = 0 \\
 &B_N(h_N, Q_N) = 0
 \end{aligned}
 \tag{4.42}$$

where the B function represents the boundary conditions and the C and M functions represent respectively the Continuity Equation (4.22) and the Momentum Equation (4.23) applied to each grid. Thus, if there are N-1 grids and two boundaries, a total of 2N equations are included in Equations (4.42). The terms within the parenthesis are the unknown variables h and Q at time level j+1.

A generalized functional iterative method known as the Newton-Raphson method [Isaacson, 1966] first used by Amein and Fang [1970], can be used to obtain an efficient solution to the non-linear system. The development of the Newton-Raphson method for a general system of non-linear equations is described in Appendix B and is quite similar to the more commonly known Newton-Raphson method of solving a single non-linear equation as described in Appendix A.

The system of 2N non-linear equations with 2N unknowns is solved by applying the Newton-Raphson method. Computations are begun by assigning trial values to the 2N unknowns. Substitution of the trial values into the system of non-linear equations yields a set of 2N residuals. A residual is the value of the right-hand side of the equation after the trial value is substituted in Equations (4.42). Solutions to

Equations (4.42) are obtained when the trial values converge to the actual values. This is accomplished by adjusting the trial values until each residual vanishes or is reduced to a tolerable quantity. Convergence is also obtained when successive trial values of the discharge and stage unknowns differ by less than a quantity known as the convergence criterion, ϵ . Actually, the discharges $(Q_i^{j+1}, Q_{i+1}^{j+1})$ have one specified convergence criterion ϵ_Q and the water surface elevations $(h_i^{j+1}, h_{i+1}^{j+1})$ have another convergence criterion ϵ_h . The Newton-Raphson method provides the means for correcting the trial values in a series of iteration steps until the residuals are reduced to tolerable values.

If only one iteration step is performed at each Δt time step, i.e., the first approximation is corrected only once, the non-linear formulation of the finite difference approximation of the Saint-Venant equations degenerates to the equivalent of a linear finite difference formulation such as used by Chen and Simons [1975]. The use of only one iteration (correction) is advantageous when the flow change is small over the selected routing interval (Δt), where the time step is selected by considerations of fixed data input or output intervals such as used in forecasting. When the time step can be selected independent of these considerations, the computational advantage of a linear solution procedure is negated by increasing the time step used in the non-linear solution beyond that needed in the linear solution to produce a desired accuracy.

In order to illustrate the Newton-Raphson method, let it be assumed that the computations have been carried through the k -th iteration cycle so that values of the unknowns have been approximated through the k -th cycle. It is desired to approximate the values of the $2N$ unknowns through the $(k+1)$ -th cycle. Let the residuals be represented by $RB_1^k, RC_1^k, RM_1^k \dots RC_i^k, RM_i^k \dots RC_{N-1}^k, RM_{N-1}^k, RB_N^k$ in which $RB, RC,$ and RM are associated with the functions $B, C,$ and $M,$ respectively. The values of the residuals at the k -th iteration cycle are:

$$\begin{aligned}
 B_1 (h_1^k, Q_1^k) &= RB_1^k \\
 C_1 (h_1^k, Q_1^k, h_2^k, Q_2^k) &= RC_1^k \\
 M_1 (h_1^k, Q_1^k, h_2^k, Q_2^k) &= RM_1^k \\
 &\dots\dots\dots \\
 C_i (h_i^k, Q_i^k, h_{i+1}^k, Q_{i+1}^k) &= RC_i^k \\
 M_i (h_i^k, Q_i^k, h_{i+1}^k, Q_{i+1}^k) &= RM_i^k
 \end{aligned}
 \tag{4.43}$$

.....

(4.43--con.)

$$C_{N-1} (h_{N-1}^k, Q_{N-1}^k, h_N^k, Q_N^k) = RC_{N-1}^k$$

$$M_{N-1} (h_{N-1}^k, Q_{N-1}^k, h_N^k, Q_N^k) = RM_{N-1}^k$$

$$B_N (h_N^k, Q_N^k) = RB_N^k$$

The residuals and the partial derivatives of the system of Equations (4.42) are related according to the Newton-Raphson algorithm, developed in Appendix B, by the following:

$$\frac{\partial B_1}{\partial h_1} dh_1 + \frac{\partial B_1}{\partial Q_1} dQ_1 = -RB_1^k$$

$$\frac{\partial C_1}{\partial h_1} dh_1 + \frac{\partial C_1}{\partial Q_1} dQ_1 + \frac{\partial C_1}{\partial h_2} dh_2 + \frac{\partial C_1}{\partial Q_2} dQ_2 = -RC_1^k$$

$$\frac{\partial M_1}{\partial h_1} dh_1 + \frac{\partial M_1}{\partial Q_1} dQ_1 + \frac{\partial M_1}{\partial h_2} dh_2 + \frac{\partial M_1}{\partial Q_2} dQ_2 = -RM_1^k$$

.....

$$\frac{\partial C_i}{\partial h_i} dh_i + \frac{\partial C_i}{\partial Q_i} dQ_i + \frac{\partial C_i}{\partial h_{i+1}} dh_{i+1} + \frac{\partial C_i}{\partial Q_{i+1}} dQ_{i+1} = -RC_i^k$$

$$\frac{\partial M_i}{\partial h_i} dh_i + \frac{\partial M_i}{\partial Q_i} dQ_i + \frac{\partial M_i}{\partial h_{i+1}} dh_{i+1} + \frac{\partial M_i}{\partial Q_{i+1}} dQ_{i+1} = -RM_i^k$$

.....

$$\frac{\partial C_{N-1}}{\partial h_{N-1}} dh_{N-1} + \frac{\partial C_{N-1}}{\partial Q_{N-1}} dQ_{N-1} + \frac{\partial C_{N-1}}{\partial h_N} dh_N + \frac{\partial C_{N-1}}{\partial Q_N} dQ_N = -RC_{N-1}^k$$

$$\frac{\partial M_{N-1}}{\partial h_{N-1}} dh_{N-1} + \frac{\partial M_{N-1}}{\partial Q_{N-1}} dQ_{N-1} + \frac{\partial M_{N-1}}{\partial h_N} dh_N + \frac{\partial M_{N-1}}{\partial Q_N} dQ_N = -RM_{N-1}^k$$

$$\frac{\partial B_N}{\partial h_N} dh_N + \frac{\partial B_N}{\partial Q_N} dQ_N = -RB_N^k$$

(4.44)

Equations (4.44) are a system of 2N linear equations with 2N unknowns [(dh_i, dQ_i) i=1,N]. Any standard method for solving a linear system of equations such as Gaussian elimination or matrix inversion can be

used for its solution. However, since the coefficient matrix denoted as the Jacobian in Appendix B consisting of the partial derivative terms of Equations (4.44) is a sparse-matrix with a band width of at most four components along the main diagonal of the matrix, as illustrated in Appendix C, a very efficient solution technique developed by Fread [1971c] and described in Appendix C is used to minimize the required computer computation time and storage.

The solution of Equations (4.44) will provide values of dh_i and dQ_i . Then, the values of the unknowns at the $(k+1)$ -th iteration cycle are obtained from the following relationships:

$$h_i^{k+1} = h_i^k + dh_i \quad (4.45)$$

$$Q_i^{k+1} = Q_i^k + dQ_i \quad (4.46)$$

The procedure is applied as many times as desired until the difference between values of any unknown in two consecutive iteration cycles is less than the appropriate convergence criterion, ϵ_h or ϵ_Q .

The terms in Equations (4.44) consist of three categories. The first is the unknowns $[(dh_i, dQ_i), i=1, N]$. The second is the residuals, which are noted to have a negative sign associated with them. The residuals as indicated in Equations (4.43) are determined by substituting the values of h_i^k and Q_i^k in Equations (4.42) and computing the resultant numerical value. It is evident that the residual associated with the boundary conditions given by Equations (4.33), (4.34), (4.36), or (4.37) is zero, while the residual of Equations (4.38)-(4.41) may be non-zero. The last category of terms is the partial derivatives. These are evaluated for the C_i and M_i functions according to the following expressions:

$$\frac{\partial C_i}{\partial h_i} = \frac{\Delta x_i}{2\Delta t_j} (B + B_o)_i^{j+1} \quad (4.47)$$

$$\frac{\partial C_i}{\partial Q_i} = -\theta \quad (4.48)$$

$$\frac{\partial C_i}{\partial h_{i+1}} = \frac{\Delta x_i}{2\Delta t_j} (B + B_o)_{i+1}^{j+1} \quad (4.49)$$

$$\frac{\partial C_i}{\partial Q_{i+1}} = \theta \quad (4.50)$$

where B_0 is the top width of the off-channel dead storage cross-sectional area:

$$\begin{aligned} \frac{\partial M_i}{\partial h_i} = \Theta \left[\left(\frac{\beta Q^2 B}{A^2} \right)_i^{j+1} + g A_i^{j+1} \left(-1 + \frac{\partial \bar{S}_f}{\partial h_i} \Delta x_i + \frac{\partial \bar{S}_e}{\partial h_i} \Delta x_i \right) \right. \\ \left. + \frac{g B_i^{j+1}}{2} \left(h_{i+1}^{j+1} - h_i^{j+1} + \bar{S}_{f_i}^{j+1} \Delta x_i + \bar{S}_{e_i}^{j+1} \Delta x_i \right) + \left(\frac{W_f dB}{2 dh} \right)_i^{j+1} \Delta x_i \right] \quad (4.51) \end{aligned}$$

$$\frac{\partial M}{\partial Q_i} = \left(\frac{\Delta x_i}{2 \Delta t_j} \right) + \Theta \left[-2 \left(\frac{\beta Q}{A} \right)_i^{j+1} + g A_i^{j+1} \left(\frac{\partial \bar{S}_f}{\partial Q_i} \Delta x_i + \frac{\partial \bar{S}_e}{\partial Q_i} \Delta x_i \right) \right] \quad (4.52)$$

$$\begin{aligned} \frac{\partial M}{\partial h_{i+1}} = \Theta \left[- \left(\frac{\beta Q^2 B}{A^2} \right)_{i+1}^{j+1} + g A_i^{j+1} \left(1 + \frac{\partial \bar{S}_f}{\partial h_{i+1}} \Delta x_i + \frac{\partial \bar{S}_e}{\partial h_{i+1}} \Delta x_i \right) \right. \\ \left. + \frac{g B_{i+1}^{j+1}}{2} \left(h_{i+1}^{j+1} - h_i^{j+1} + \bar{S}_{f_i}^{j+1} \Delta x_i + \bar{S}_{e_i}^{j+1} \Delta x_i \right) + \left(\frac{W_f dB}{2 dh} \right)_{i+1}^j \Delta x_i \right] \quad (4.53) \end{aligned}$$

$$\frac{\partial M}{\partial Q_{i+1}} = \left(\frac{\Delta x_i}{2 \Delta t_j} \right) + \Theta \left[2 \left(\frac{\beta Q}{A} \right)_{i+1}^{j+1} + g A_i^{j+1} \left(\frac{\partial \bar{S}_f}{\partial Q_{i+1}} \Delta x_i + \frac{\partial \bar{S}_e}{\partial Q_i} \Delta x_i \right) \right] \quad (4.54)$$

in which:

$$\frac{\partial \bar{S}_f}{\partial h_i} = 2 \bar{S}_{f_i} \left(\frac{d\bar{n}/dh_i}{\bar{n}_i} - \frac{5B_i}{6\bar{A}} + \frac{dB_i/dh_i}{3\bar{B}} \right) \quad (4.55)$$

$$\frac{\partial \bar{S}_f}{\partial h_{i+1}} = 2 \bar{S}_{f_i} \left(\frac{d\bar{n}/dh_{i+1}}{\bar{n}_i} - \frac{5B_{i+1}}{6\bar{A}} + \frac{dB_{i+1}/dh_{i+1}}{3\bar{B}} \right) \quad (4.56)$$

$$\frac{\partial \bar{S}_f}{\partial Q_i} = 2 \bar{S}_{f_i} \left(\frac{d\bar{n}/dQ_i}{\bar{n}_i} + \frac{1}{2Q} \right) \quad (4.57)$$

$$\frac{\partial \bar{S}_f}{\partial Q_{i+1}} = 2 \bar{S}_{f_i} \left(\frac{d\bar{n}/dQ_{i+1}}{\bar{n}_i} + \frac{1}{2Q} \right) \quad (4.58)$$

$$\frac{\partial \bar{S}_e}{\partial h_i} = \frac{2 \bar{S}_{e_i} B_i V_i^2}{A_i (V_{i+1}^2 - V_i^2)} \quad (4.59)$$

$$\frac{\partial \bar{S}_e}{\partial h_{i+1}} = \frac{-2 \bar{S}_{e_i} B_{i+1} V_{i+1}^2}{A_{i+1} (V_{i+1}^2 - V_i^2)} \quad (4.60)$$

$$\frac{\partial \bar{S}_e}{\partial Q_i} = \frac{-2 \bar{S}_{e_i} V_i}{(V_{i+1}^2 - V_i^2) A_i} \quad (4.61)$$

$$\frac{\partial \bar{S}_e}{\partial Q_{i+1}} = \frac{2 \bar{S}_{e_i} V_{i+1}}{(V_{i+1}^2 - V_i^2) A_{i+1}} \quad (4.62)$$

where:

$$dB_i/dh_i = \Delta B_i / \Delta h_i \quad (4.63)$$

$$V_i = Q_i / A_i \quad (4.64)$$

$$V_{i+1} = Q_{i+1} / A_{i+1} \quad (4.65)$$

$$d\bar{n}/dh_i = \frac{\Delta \bar{n} d\hat{h}}{\Delta \hat{h} dh_i} \quad (4.66)$$

$$d\bar{n}/dQ_i = \frac{\Delta \bar{n} d\hat{Q}}{\Delta \hat{Q} dQ_i} \quad (4.67)$$

$$\hat{h} = \frac{h_m + h_{m+1}}{2} \quad (4.68)$$

$$\hat{Q} = \frac{Q_m + Q_{m+1}}{2} \quad (4.69)$$

and

$$\left. \begin{aligned} d\hat{h}/dh_i &= 0 && \text{if } i \neq m \\ d\hat{h}/dh_i &= 1/2 && \text{if } i = m \end{aligned} \right\} \quad (4.70)$$

$$\left. \begin{aligned} d\hat{Q}/dQ_i &= 0 && \text{if } i \neq m \\ d\hat{Q}/dQ_i &= 1/2 && \text{if } i = m \end{aligned} \right\} \quad (4.71)$$

Whereas the i and $i+1$ subscripts in Equations (4.47)-(4.71) denote each node location along the routing reach, the m and $m+1$ subscripts denote the upstream and downstream node locations between which the Manning \bar{n} relationship with stage or discharge is considered constant with respect to distance along the routing reach.

The partial derivatives for the B_1 and B_N functions are evaluated as follows:

$$\frac{\partial B_1}{\partial h_1} = 1 \quad (4.72)$$

$$\frac{\partial B_1}{\partial Q_1} = 0 \quad (4.73)$$

when the upstream boundary is a stage hydrograph, Equation (4.33), or:

$$\frac{\partial B_1}{\partial h_1} = 0 \quad (4.74)$$

$$\frac{\partial B_1}{\partial Q_1} = 1 \quad (4.75)$$

when the upstream boundary is a discharge hydrograph, Equation (4.34), and:

$$\frac{\partial B_N}{\partial h_N} = 1 \quad (4.76)$$

$$\frac{\partial B_N}{\partial Q_N} = 0 \quad (4.77)$$

when the downstream boundary is a stage hydrograph, Equation (4.36), or:

$$\frac{\partial B_N}{\partial h_N} = 0 \quad (4.78)$$

$$\frac{\partial B_N}{\partial Q_N} = 1 \quad (4.79)$$

when the downstream boundary is a discharge hydrograph, Equation (4.37), or:

$$\frac{\partial B_N}{\partial h_N} = - \frac{(Q_{k+1} - Q_k)}{(h_{k+1} - h_k)} \quad (4.80)$$

$$\frac{\partial B_N}{\partial Q_N} = 1 \quad (4.81)$$

when the downstream boundary is a stage-discharge single value rating curve, Equation (4.39), or:

$$\begin{aligned} \frac{\partial B_N}{\partial h_N} = & \left[-1.486 \left(\frac{AR^{2/3}}{n} \right)_N^{j+1} \left(\frac{h_{N-1}^{j+1} - h_N^{j+1}}{\Delta x_{N-1}} \right)^{1/2} \right] \left[\frac{-dn/dh_N}{n_N} + \frac{5}{3} \left(\frac{B}{A} \right)_N^{j+1} \right. \\ & \left. - \frac{2}{3} \left(\frac{dB/dh}{B} \right)_N^{j+1} - \frac{1}{2(h_{N-1}^{j+1} - h_N^{j+1})} \right] \end{aligned} \quad (4.82)$$

$$\frac{\partial B_N}{\partial Q_N} = 1 \quad (4.83)$$

when the downstream boundary is a stage-discharge loop rating curve, Equation (4.40), or:

$$\frac{\partial B_N}{\partial h_N} = -ab(h_N^{j+1} - h_w)^{b-1} \quad (4.84)$$

$$\frac{\partial B_N}{\partial Q_N} = 1 \quad (4.85)$$

when the downstream boundary is a weir type stage-discharge relation, Equation (4.41).

Relaxation Algorithm for System of Rivers

The implicit formulation of the Saint-Venant equations is well suited for simulating unsteady flows in a system of rivers such as the one shown in Fig. 4.7, since the response of the system as a whole is determined for each time step. Also, because the implicit technique is stable for large time steps, it can provide an efficient means of obtaining the transient response of river systems subjected to floods of several days' or even weeks' duration.

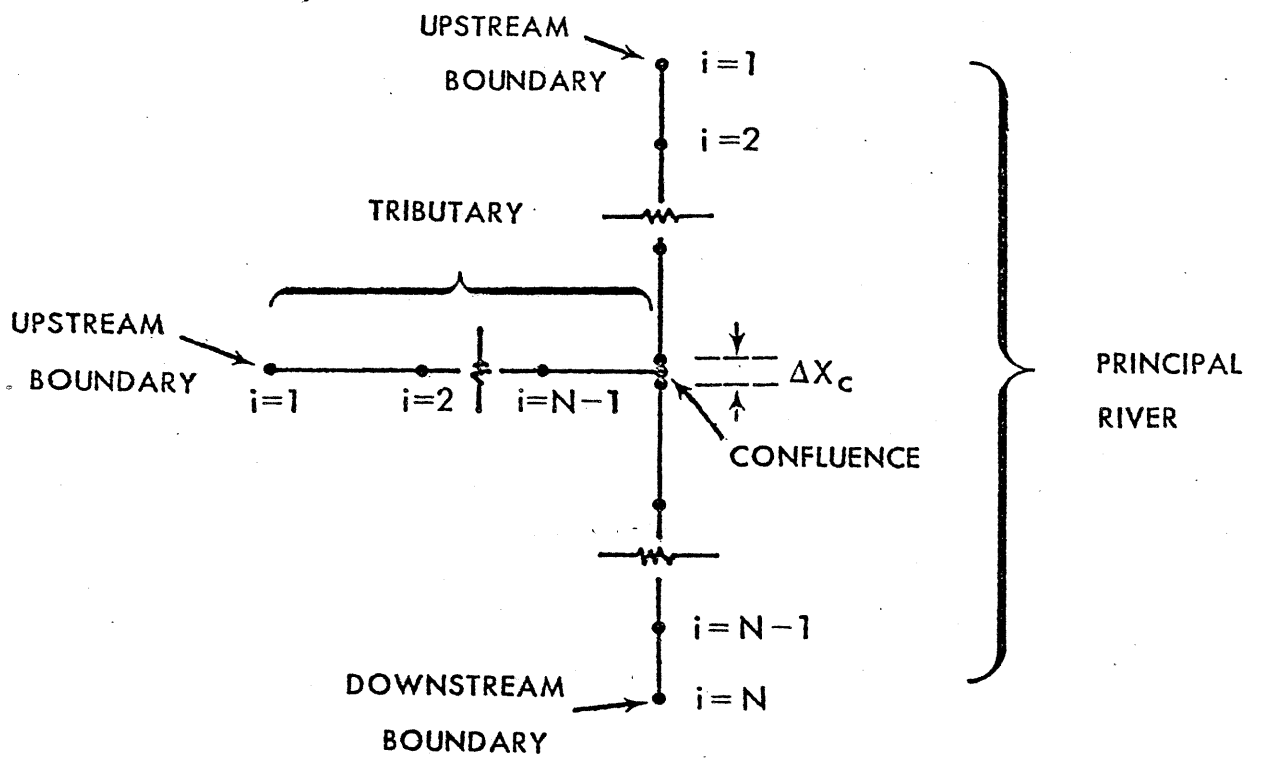


Fig. 4.7.--Application of implicit solution technique to system of rivers.

The following criteria should be considered in developing a technique for applying the implicit method of dynamic routing to a river system: (1) the continuous storage and dynamic interactions at the confluence of the tributary and the principal (main stem) river must be properly simulated; (2) an efficient matrix solution algorithm such as presented in Appendix C must be used; and (3) the technique must be adaptable to a river with several tributaries. An algorithm satisfying the above criteria can be devised by applying the implicit technique to one river at a time and the separate transient responses so obtained are coupled by conserving mass and momentum of flow in each river at the confluence. A complete conservation is accomplished by treating the tributary flow at the confluence as lateral flow q when the transient response of the principal river is obtained. (Losses at the confluence other than friction are not considered.) Since the tributary flow depends in part on the water surface elevation at the confluence, and vice versa, an iterative or relaxation procedure is necessary. The application of the implicit technique of dynamic flood routing to the river system shown in Fig. 4.7 is summarized by the following algorithm [Fread, 1973c].

1. Specify the initial conditions and the upstream boundary condition for the principal river and the tributary; specify the downstream boundary condition for the principal river.

2. Estimate the tributary flow Q_{te} occurring at the confluence for the time $t+\Delta t$.

3. Solve the implicit difference Equations (4.22) and (4.23) for the principal river by using a lateral inflow $Q_{te}/\Delta x_c$ along the finite reach Δx_c (the width of the tributary); the solution obtained for the water surface elevation at the midpoint of Δx_c is denoted as h_c .

4. Solve the implicit difference Equations (4.22) and (4.23) for the tributary by using h_c as the downstream boundary condition; the solution obtained for the tributary flow at the downstream boundary is denoted as Q_{ts} .

5. If $|Q_{te} - Q_{ts}| < \epsilon_c$, a predetermined error tolerance, increment the time and return to step 2; otherwise:

$$Q_{te} = \alpha_c Q_{ts} + (1 - \alpha_c) Q_{te} \quad (4.86)$$

where α_c is a weighting factor ($0.5 \leq \alpha_c \leq 1.0$) and return to step 3.

The rate of convergence of the algorithm can be increased by using parabolic extrapolation to obtain Q_{te} in step 2. The convergence can be accelerated further by a proper selection of the weighting factor α_c . Usually, one to two iterations is required for convergence when a reasonable value of the error tolerance ϵ_c is used.

REFERENCES

- Abbott, M. B., Ionescu, F., 1967: On the numerical computation of nearly horizontal flows. J. Hydraul. Res., 5(2), 97-117.
- Amein, M., 1966: Streamflow routing on computer by characteristics. Water Resour. Res., 2(1), 123-130.
- Amein, M., 1968: An implicit method for numerical flood routing. Water Resour. Res., 4(4), 719-726.
- Amein, M., and Fang, C. S., 1969: Streamflow routing (with application to North Carolina rivers). Report No. 17, Water Resour. Res. Inst. of the Univ. of North Carolina, Raleigh, N.C.
- Amein, M., and Fang, C.S., 1970: Implicit flood routing in natural channels. J. Hydraul. Div. Amer. Soc. Civil Eng., 96(HY12), 2481-2500.
- Amein, M., 1975: Computation of flow through Masonboro Inlet, N.C. J. Waterways, Harbors, and Coastal Eng. Div. Amer. Soc. Civil Eng., 101(WW1), 93-108.
- Amein, M., and Chu, H. L., 1975: Implicit numerical modeling of unsteady flows. J. Hydraul. Div. Amer. Soc. Civil Eng., 101(HY6), 717-731.
- Balloffet, A., 1969: One-dimensional analysis of floods and tides in open channels. J. Hydraul. Div. Amer. Soc. Civil Eng., 95(HY4), 1429-1451.
- Baltzer, R. A., and Lai, C., 1968: Computer simulation of unsteady flows in water-ways. J. Hydraul. Div. Amer. Soc. Civil Eng., 94(HY4), 1083-1117.
- Barré De Saint-Venant, 1871: Theory of unsteady water flow, with application to river floods and to propagation of tides in river channels. French Academy of Science, 73, 148-154, 237-240.
- Chaudhry, Y. M., and Contractor, D. N., 1973: Application of implicit method to surges in channels. Water Resour. Res., 9(6), 1605-1612.
- Chen, Y. H. (University of California, Davis) 1973: Mathematical modeling of water and sediment routing in natural channels. Ph. D. Dissertation, 252 pp.
- Chen, Y. H., and Simons, D. B., 1975: Mathematical modeling of alluvial channels. Modeling 75 Symposium on Modeling Techniques, Second Annual Symposium of Waterways, Harbors, and Coastal Eng. Div. Amer. Soc. Civil Eng., September 1975, Vol. 1, 466-483.

- Chow, Ven T., 1959: Open-channel hydraulics. McGraw-Hill, New York, N.Y., 680 pp.
- Conte, S. D., 1965: Elementary numerical analysis. McGraw-Hill, New York, N.Y., 278 pp.
- Contractor, D. N., and Wiggert, J. M., 1972: Numerical studies of unsteady flow in the James River. Bulletin 51, VPI-WRRC-Bull 51, Water Resour. Res. Ctr., Virginia Poly Inst. and State Univ., Blacksburg, Va., 56 pp.
- Courant, R., and Friedrichs, K. O., 1948: Supersonic flow and shock waves. Interscience Publishers, Inc., New York.
- Dronkers, J. J., 1969: Tidal computations for rivers, coastal areas, and seas. J. Hydraul. Div. Amer. Soc. Civil Eng., 95 (HY1), 29-77.
- Ellis, John, 1970: Unsteady flow in channel of variable cross section. J. Hydraul. Div. Amer. Soc. Civil Eng., 96 (HY10), 1927-1945.
- Fletcher, F. Alan, and Hamilton, Wallis S., 1967: Flood routing in an irregular channel. J. Eng. Mech. Div. Amer. Soc. Civil Eng., 93(EM3), 45-62.
- Fread, D. L., and Harbaugh, T. E., 1971a: Numerical simulation of transient open-channel flow. Civil Eng. Studies, Univ. of Missouri-Rolla, Rolla, Mo., 204 pp.
- Fread, D. L., and Harbaugh, T. E., 1971b: Gradually varied flow profiles by Newton's iteration technique. J. Hydrol., 2, 129-139.
- Fread, D. L., 1971c: Discussion of implicit flood routing in natural channels. M. Amein and C. S. Fang, J. Hydraul. Div. Amer. Soc. Civil Eng., 97 (HY7), 1156-1159.
- Fread, D. L., and Harbaugh, T. E., 1973a: Transient hydraulic simulation of breached earth dams. J. Hydraul. Div. Amer. Soc. Civil Eng., 99 (HY1), 139-154.
- Fread, D. L., 1973b: Effect of time step size in implicit dynamic routing. Water Resour. Bull., 9(2), 338-351.
- Fread, D. L., 1973c: Technique for implicit dynamic routing in rivers with major tributaries. Water Resour. Res., 9(4), 918-926.
- Fread, D. L., 1973d: A dynamic model of stage-discharge relations affected by changing discharge. NOAA Technical Memorandum NWS HYDRO-16, National Weather Service, National Oceanic and Atmospheric Administration, U.S. Department of Commerce, Silver Spring, Md., 51 pp.

- Fread, D. L., 1974a: Numerical properties of implicit four-point finite difference equations of unsteady flow. NOAA Technical Memorandum NWS HYDRO-18, National Weather Service, National Oceanic and Atmospheric Administration, U.S. Department of Commerce, Silver Spring, Md., 38 pp.
- Fread, D. L., 1974b: Implicit dynamic routing of floods and surges in the Lower Mississippi. Presented at Amer. Geophys. Union National Meeting, April 1974, Washington, D.C., 26 pp.
- Fread, D. L., 1975a: Computation of stage-discharge relationships affected by unsteady flow. Water Resour. Bull., 11(2), 213-228.
- Fread, D. L., 1975b: Discussion of comparison of four numerical methods for flood routing. R. K. Price, J. Hydraul. Div. Amer. Soc. Civil Eng., 101(HY3), 565-567.
- Fread, D. L., 1976: Flood routing in meandering rivers with flood plains. Rivers '76, Symposium on Inland Waterways for Navigation, Flood Control, and Water Diversions, August 10-12, 1976, Colorado State Univ., Fort Collins, Colo., Vol. I, 16-35.
- Garrison, J. M., Granju, J. P., and Price, J. T., 1969: Unsteady flow simulation in rivers and reservoirs. J. Hydraul. Div. Amer. Soc. Civil Eng., 95(HY5), 1559-1576.
- Greco, F., and Pattattoni, L., 1975: An implicit method to solve Saint-Venant equations. J. Hydrol., 24, 171-185.
- Gunaratnam, D. J., and Perkins, F. E., 1970: Numerical solution of unsteady flows in open channels. Hydrodynamics Lab Rep. 127, Department of Civil Eng., Mass. Inst. of Tech., Cambridge, Mass., 260 pp.
- Henderson, F. M., 1966: Open channel flow. Macmillan Co., New York, 521 pp.
- Isaacson, E., Stoker, J. J., and Troesch, A., 1954, 1956: Numerical solution of flood prediction and river regulation problems. Rep. IMM-205, IMM-235, Inst. for Math. and Mech., New York Univ., New York, 47 pp, 70 pp.
- Isaacson, E., Stoker, J. J., and Troesch, A., 1958: Numerical solution of flow problems in rivers. J. Hydraul. Div. Amer. Soc. Civil Eng., 84(HY5), pp. 1810-1 - 1810-13.
- Isaacson, E., and Keller, H. B., 1966: Analysis of numerical methods. John Wiley and Sons, New York, 531 pp.

- Isaacson, E., 1966: Fluid dynamical calculations. Numerical solution of partial differential equations. Academic Press, Inc., New York, N.Y., 35-49.
- Johnson, B., 1974: Unsteady flow computations on the Ohio-Cumberland-Tennessee-Mississippi River System, Tech. Rep. H-74-8, Hydr. Lab. U.S. Army Eng. Waterways Exper. Sta., Vicksburg, Miss., 44 pp.
- Kamphuis, J. W., 1970: Mathematical tidal study of St. Lawrence River, J. Hydraul. Div. Amer. Soc. Civil Eng., 96 (HY3), 643-664.
- Leendertse, J. J., 1967: Aspects of a computational model for long-period water-wave propagation. Rand Memorandum RM-5294-PR, Rand Corp., Santa Monica, Calif., 165 pp.
- Liggett, J. A., and Woolhiser, D. A., 1967: Difference solutions of the shallow-water equations. J. Eng. Mech. Div. Amer. Soc. Civil Eng., 95(EM2), 39-71.
- Liggett, J. A., 1975: Basic equations of unsteady flow. Unsteady flow in open channels. Edited by K. Mahmood and V. Yevjevich, Vol. I, Chap. 3, Water Resour. Pub., Ft. Collins, Colo., 29-62.
- Liggett, J. A., and Cunge, J. A., 1975: Numerical methods of solution of the unsteady flow equations. Unsteady flow in open channels. Edited by K. Mahmood and V. Yevjevich, Vol. I, Chap. 4, Water Resour. Pub., Ft. Collins, Colo., 89-182.
- Martin, C. S., and De Fazio, F. G., 1969: Open channel surge simulation by digital computer. J. Hydraul. Div. Amer. Soc. Civil Eng., 95 (HY6), 2049-2070.
- O'Brien, G. G., Hyman, M. A., and Kaplan, S., 1951: A study of the numerical solution of partial differential equations. J. Math. and Phys., 29(4), 223-251.
- Prandle, D., and Crookshank, N. L., 1974: Numerical model of St. Lawrence River estuary, J. Hydraul. Div. Amer. Soc. Civil Eng., 100 (HY4), 517-529.
- Preissmann, A., 1961: Propagation of translatory waves in channels and rivers. 1st Congres de l'Assoc. Francaise de Calcul, Grenoble, France, 433-442.
- Preissman, A., and Cunge, J. A., 1961: Tidal bore calculation on an electronic computer. La Houille Blanche, 5, 588-596.
- Quinn, F. H., and Wylie, E. B., 1972: Transient analysis of the Detroit River by the implicit method. Water Resour. Res., 8(6), 1461-1469.

- Ragan, Robert M. (Cornell University, Ithaca, New York) 1965: Synthesis of hydrographs and water surface profiles for unsteady open channel flow with lateral inflows. Ph. D. Dissertation.
- Richtmyer, R. D., 1962: A survey of difference methods for non-steady fluid dynamics. NGAR Technical Notes 63-2, National Center for Atmospheric Research, Boulder, Colo., 234 pp.
- Stoker, J. J., 1953: Numerical solution of flood prediction and river regulation problems. Rep. IMM-200, Inst. for Math, and Mech., New York Univ., New York, 36 pp.
- Stoker, J. J., 1957: Water waves. Interscience, New York, 567 pp.
- Streeter, V. L., and Wylie, E. B., 1967: Hydraulic transients. Chap. 15, McGraw-Hill, New York, N.Y., 329 pp.
- Strelkoff, T., 1969: The one-dimensional equations of open-channel flow. J. Hydraul. Div. Amer. Soc. Civil Eng., 95 (HY3), 861-874.
- Strelkoff, T., 1970: Numerical solution of Saint-Venant equations. J. Hydraul. Div. Amer. Soc. Civil Eng., 96 (HY1), 223-252.
- Terzidis, George (University of California, Davis) 1968: Discontinuous unsteady flow in open channels. Ph. D. Dissertation, 105 pp.
- Vasiliev, O. F., Gladyshev, M. T., Pritvits, N. A., and Sudobicher, V. G., 1965: Numerical methods for the calculation of shock wave propagation in open channels. Proceedings International Association for Hydraulic Research, Eleventh International Congress, 44(3), Leningrad, U.S.S.R., 14 pp.
- Wylie, E. G., 1970: Unsteady free-surface flow computations. J. Hydraul. Div. Amer. Soc. Civil Eng., 96 (HY11), 2241-2251.

APPENDIX A

SOLUTION OF NON-LINEAR EQUATION BY NEWTON-RAPHSON ITERATION

A non-linear equation may be solved by a functional iterative technique such as Newton-Raphson Iteration. Consider the following equation expressed in functional form:

$$f(x) = 0 \tag{A.1}$$

Non-linearity arises when the equation contains the variable x raised to any power other than unity. The solution of Equation (A.1) is obtained in an iterative manner, proceeding from a first solution estimate x^k towards succeeding improved estimates x^{k+1} , which tend to converge toward the solution denoted as X in Fig. A.1. The orderly procedure by which the improved solution estimate x^{k+1} is obtained so that it converges to an acceptable solution is known as Newton-Raphson Iteration [Conte, 1967; Fread, 1971b] and is described as follows.

A non-linear equation such as Equation (A.1) may be linearized by using only the first two terms of its Taylor series expansion at x^k , i.e.,

$$f(x) = f(x^k) + f'(x^k) (x - x^k) \tag{A.2}$$

where the prime (') denotes a derivative evaluated at x^k , i.e., $f'(x) = df(x)/dx$. The right side of Equation (A.2) is the linear function of x^k that best approximates the non-linear function $f(x)$ which is evaluated at x^k . An iterative procedure, which will cause $f(x^k)$ to approach zero as the quantity $(x-x^k)$ approaches zero, can be obtained from Equation (A.2) by setting $f(x)$ equal to zero and replacing x with x^{k+1} , which will be an improved solution estimate for x if the iterative procedure is convergent. Hence, Equation (A.2) takes the form:

$$x^{k+1} = x^k - f(x^k)/f'(x^k) \tag{A.3}$$

where the k superscript denotes the number of iteration.

Equation (A.3), the general iteration algorithm of Newton, is repeated until the difference $(x^{k+1} - x^k)$ is less than ϵ_1 , or until $f(x^k)$ is less than ϵ_2 . When either occurs, the iteration process has converged; i.e., x^{k+1} has approached X to within the prescribed error tolerance ϵ_1 or ϵ_2 . The case of convergence according to the ϵ_2 criterion is illustrated in Fig. A.1.

The convergence of the iteration process depends on a good first solution estimate $x^{k=1}$. If the estimate is sufficiently close to X , convergence is attained; and it is at a quadratic rate, i.e., second order, since the iterative procedure involves the first derivative.

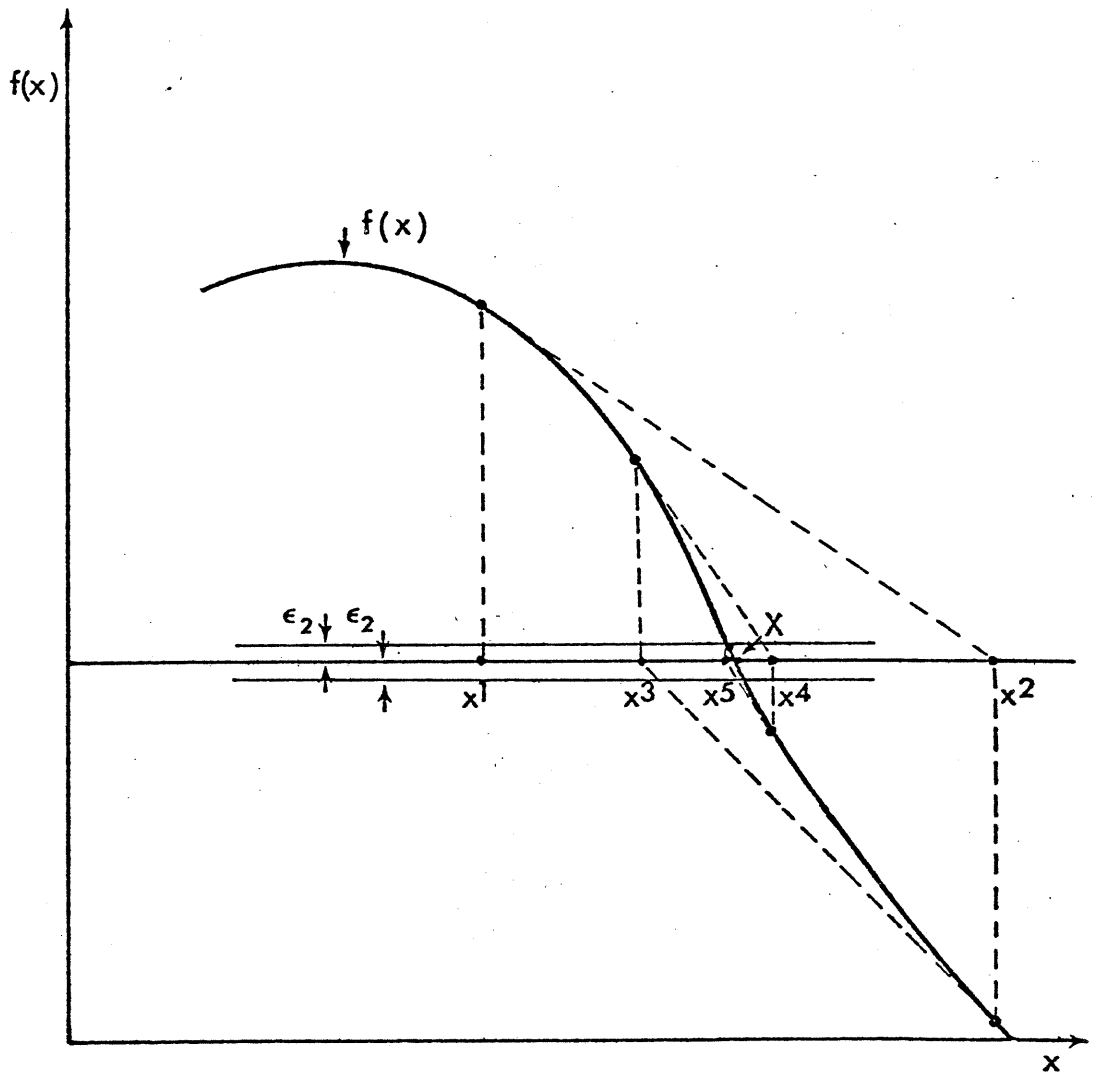


Fig. A.1.—Graphical illustration of convergence process of Newton-Raphson iteration.

The non-linear equations which are solved by the Newton-Raphson iterative algorithm in this report are time dependent finite-difference equations. A first estimate of the solution is obtained by using the solution associated with the time $t-\Delta t$. Using this as the initial estimate, the iteration process will converge. The convergence process can be hastened when the first solution estimate $x^{k=1}$ is made closer to the acceptable solution. A simple linear extrapolation is used to provide better first solution estimates. Thus:

$$x_j^{k=1} = x_{j-1} + \alpha(x_{j-1} - x_{j-2}) \quad (\text{A.4})$$

where the j subscript denotes the solution at time t and $j-1$ denotes the solution at time $t-\Delta t$, etc. The weighting factor α varies from zero to unity. A value of 0.5 is usually a safe value which will insure convergence within a few iterations.

APPENDIX B

SOLUTION OF NON-LINEAR SYSTEM OF EQUATIONS BY NEWTON-RAPHSON ITERATION

A system of non-linear algebraic equations may be solved simultaneously by a functional iterative technique known as Newton-Raphson Iteration [Isaacson and Keller, 1966]. Consider the following M-dimensional system of non-linear algebraic equations:

$$\begin{matrix} f_1(x_1^j, x_2^j \dots \dots \dots x_M^j) = 0 \\ \vdots \\ f_M(x_1^j, x_2^j \dots \dots \dots x_M^j) = 0 \end{matrix} \quad (B.1)$$

or in vector notation:

$$f(\vec{X}^j) = 0 \quad (B.2)$$

The superscript j denotes a particular system of equations. When the algebraic non-linear equations emanate from finite difference approximations of time dependent partial differential equations, j denotes the particular time level at which solutions to the differential equations are sought.

The solution vector \vec{X}^j of Equation (B.1) is obtained in an iterative manner, proceeding from a first solution estimate \vec{X}^k towards succeeding improved estimates \vec{X}^{k+1} , which tend to converge toward the solution vector \vec{X}^j . The orderly procedure by which the improved solution estimate \vec{X}^{k+1} is obtained such that it converges toward \vec{X}^j is known as Newton-Raphson Iteration and may be described as follows.

The non-linear system $f(\vec{X})$ may be linearized by using the first two terms of its Taylor Series expansion at \vec{X}^k , i.e.,

$$f(\vec{X}^j) \approx f(\vec{X}^k) + \sum_{i=1}^M f'_i(\vec{X}^k) (\vec{X}_i^j - \vec{X}_i^k) \quad (B.3)$$

where:

$$f'_i(\vec{X}^k) = \frac{\partial f(\vec{X}^k)}{\partial X_i} \quad (B.4)$$

Equation (B.3) may be expressed in a concise form as:

$$f(\vec{X}^j) \approx f(\vec{X}^k) + \underline{J}'(\vec{X}^k) \Delta \vec{X} \quad (B.5)$$

where $\underline{J}'(\vec{X}^k)$ is the Jacobian, a coefficient matrix made up of the partial derivatives evaluated at \vec{X}^k , and $\Delta \vec{X}$ is a correction term

defined as:

$$\vec{\Delta X} = \vec{X}_i^j - \vec{X}_i^k \quad (\text{B.6})$$

The right-hand side of Equation (B.5) is the linear vector function of \vec{X}^k that best approximates the non-linear function $f(\vec{X})$, evaluated at \vec{X}^k . An iterative procedure is desired which will cause the vector function $f(\vec{X}^k)$ to approach zero as $\vec{\Delta X}$, the correction vector, approaches zero. Therefore, the right-hand side of Equation (B.5) is used to construct the general iteration algorithm, i.e.,

$$J'(\vec{X}^k) \vec{\Delta X} = -f(\vec{X}^k) \quad (\text{B.7})$$

In Equation (B.7), $\vec{\Delta X}$ is now defined as the difference between an improved solution vector \vec{X}^{k+1} and the old solution vector \vec{X}^k .

The right-hand side of Equation (B.7) is the negative of the residual or error vector produced by using the solution estimate vector \vec{X}^k in Equation (B.2). The Jacobian is known since it is evaluated as \vec{X}^k .

The linear system of equations represented in vector form by Equation (B.7) may be solved for the unknown linear correction vector $\vec{\Delta X}$ by a suitable matrix solution technique. A variation of Gaussian elimination was chosen as the most efficient matrix solution technique; it is described in Appendix C.

The correction vector is used to obtain an improved solution vector estimate \vec{X}^{k+1} of the solution vector \vec{X}^j . The process is repeated until $\vec{\Delta X}$ is less than ϵ which is a suitable tolerance vector. When this occurs, the iteration process has converged, i.e., \vec{X}^{k+1} has approached \vec{X}^j within the prescribed tolerance ϵ . The convergence of the iteration process depends on a good first solution vector estimate $\vec{X}^{k=1}$. If the estimate is sufficiently close to \vec{X}^j , convergence is attained at a quadratic rate since the iterative procedure is second order (involves the first derivative).

When applying the Newton-Raphson Iteration to non-linear finite difference approximations to the Saint-Venant equations, the first estimate solution vector $\vec{X}^{k=1}$ can be chosen sufficiently close to \vec{X}^j to allow convergence. A reasonably accurate initial condition provides the first $\vec{X}^{k=1}$, and linear or parabolic extrapolated first estimates may be used thereafter. Linear extrapolations are obtained from the following expression:

$$\vec{X}^{k=1} = \vec{X}^{j-1} + \frac{\alpha \Delta t^j}{\Delta t^{j-1}} (\vec{X}^{j-1} - \vec{X}^{j-2}) \quad (\text{B.8})$$

where Δt^j and Δt^{j-1} are the values of the time steps between the time levels corresponding to the solution vectors, \vec{X}^j and \vec{X}^{j-1} , respectively.

The weighting factor α varies from zero to unity. If the time steps are constant, the following parabolic extrapolation algorithm yields parabolic extrapolations for the first estimate solution vectors:

$$\vec{x}^{k=1} = \vec{x}^{j-3} + 3(\vec{x}^{j-1} - \vec{x}^{j-2}) \quad (\text{B.9})$$

If the time steps are not constant, linear extrapolation is used for all extrapolated first estimate vectors.

5. $F = -J_{i+1,1}/J_{i-1,k+1}$ (C.8)
6. $J_{i+1,2} = F \cdot J_{i-1,k+2} + J_{i+1,2}$ (C.9)
7. $R_{i+1} = F \cdot R_{i-1} + R_{i+1}$ (C.10)
8. $F = -J_{i+1,2}/J_{i,2}$ (C.11)
9. $J_{i+1,3} = F \cdot J_{i,3} + J_{i+1,3}$ (C.12)
10. $J_{i+1,4} = F \cdot J_{i,4} + J_{i+1,4}$ (C.13)
11. $R_{i+1} = F \cdot R_i + R_{i+1}$ (C.14)
12. Set $k = 2$
13. If $i < (M-2)$ increment i by 2 and return to step 2; otherwise, proceed to step 14.
14. Set $k = 2$ and $i = M-1$
15. $F = -J_{M,3}/J_{i,3}$ (C.15)
16. $J_{M,4} = F \cdot J_{i,4} + J_{M,4}$ (C.16)
17. $R_M = F \cdot R_i + R_M$ (C.17)
18. $X_M = R_M/J_{M,4}$ (C.18)
19. $X_i = (R_i - J_{i,k+2} \cdot X_{i+1})/J_{i,k+1}$ (C.19)
20. If $i = 1$, stop; otherwise, decrease i by 1 and proceed to step 21.
21. $X_i = (R_i - J_{i,4} \cdot X_{i+2} - J_{i,3} \cdot X_{i+1})/J_{i,2}$ (C.20)
22. Decrease i by 1
23. If $i > 1$, return to step 19; otherwise, set $k = 0$ and return to step 19.

Steps 1-18 reduce the augmented matrix J/R to an upper triangular form. Steps 19-23 perform the back-substitution by which the solution vector X is obtained.